Study of the exclusive $b \to ul^- \bar{\nu}_l$ decays in the MSSM with and without R-parity violation

C. S. Kim* and Ru-Min Wang†

Department of Physics, Yonsei University, Seoul 120-479, Korea

(Received 26 December 2007; published 9 May 2008)

We study the exclusive $b \to u\ell^- \bar{\nu}_\ell (\ell = \tau, \mu, e)$ decays in the minimal supersymmetric standard model with and without R-parity violation. From the experimental measurements of branching ratios $\mathcal{B}(B_u^- \to \tau^- \bar{\nu}_\tau)$, $\mathcal{B}(B_u^- \to M'^0 \ell'^- \bar{\nu}_{\ell'})$ and $\mathcal{B}(\bar{B}_d^0 \to M'^+ \ell'^- \bar{\nu}_{\ell'})$ ($\ell' = \mu, e, M' = \pi, \rho$), we derive new upper bounds on the relevant new physics parameters within the decays. Using the constrained new physics parameter spaces, we predict the charged Higgs effects and the R-parity violating effects on the branching ratios, the normalized forward-backward asymmetries of charged leptons, and the ratios of longitudinal to transverse polarization of the vector mesons, which have not been measured or have not been well measured yet. We find that the charged Higgs effects and the R-parity violating effects could be large and measurable in some cases. Our results could be used to probe new physics effects in the leptonic decays as well as the semileptonic decays, and will correlate with searches for direct supersymmetric signals in future experiments.

DOI: 10.1103/PhysRevD.77.094006 PACS numbers: 13.20.He, 11.30.Fs, 12.60.Jv, 14.80.Cp

I. INTRODUCTION

The B decays have received a lot of attention, since they are very promising for investigating the standard model (SM) and searching for new physics (NP) beyond it. Among these B decays, the semileptonic ones have played a central role for a long time, since the most precise measurements of the Cabibbo-Kobayashi-Maskawa (CKM) matrix elements $|V_{ub}|$ and $|V_{cb}|$ are based on the semileptonic decays $b \to u\ell^- \bar{\nu}_\ell$ and $b \to c\ell^- \bar{\nu}_\ell$, respectively. These decays can also be very useful to test the various NP scenarios like the two Higgs doublet models [1], the minimal supersymmetric standard model (MSSM) [2,3], *etc*.

It is known that the charged Higgs boson exists in any models with two or more Higgs doublets, such as the MSSM which contains two Higgs doublets H_u and H_d coupling to up and down type quarks, respectively. The charged Higgs sectors of all these models may be characterized by the ratio of the two Higgs vacuum expectation values, $\tan\beta$, and the mass of the charged Higgs, m_H. Large $\tan\beta$ regime of both supersymmetric and nonsupersymmetric models has a few interesting signatures in B physics (for instance, see Refs. [4–12] and references therein). One of the most clear ones is the suppression of $\mathcal{B}(B_u^- \to \tau^- \bar{\nu}_\tau)$ with respect to its SM expectation [12]. In the MSSM, the charged Higgs contributions to the exclusive $b \to u\ell^- \bar{\nu}_\ell$ decays, including $B_u^- \to \tau^- \bar{\nu}_\tau$ decay, come from the b quark transforms to a u quark emitting a virtual charged Higgs that manifests itself as a lepton-neutrino pair. In this paper, we will present a correlated analysis of all these exclusive $b \to u\ell^- \bar{\nu}_\ell$ observables within the large $\tan\beta$ limit of the MSSM.

In the MSSM, one can introduce a discrete symmetry, called R-parity (R_p) [13], to enforce in a simple way the lepton number (L) and the baryon number (B) conservations. In view of the important phenomenological differences between supersymmetric models with and without R_p violation, it is also worth studying the extent to which R_p can be broken. The effects of supersymmetry with R_p violation in B meson decays have been extensively investigated, for instance Refs. [14–20]. In Ref. [20], the R_p violating (RPV) and lepton flavor violating coupling effects have been studied in $B^- \to \ell^- \bar{\nu}_\ell$ decays. The exclusive $b \to u\ell^- \bar{\nu}_\ell$ decays involve the same set of the RPV coupling products for every generation of leptons. In this work, still assuming lepton flavor conservation, we will investigate the sensitivity of the exclusive $b \to u\ell^- \bar{\nu}_\ell$ decays to the RPV coupling contributions in the RPV MSSM, too.

The paper is organized as follows. In Sec. II, we introduce the theoretical frame of the exclusive $b \to u\ell^- \bar{\nu}_\ell$ decays in the MSSM with and without R_p violation in detail. In Sec. III, we tabulate all the theoretical inputs. In Secs. IV and V, we deal with the numerical results. We display the constrained parameter spaces which satisfy all the available experimental data, and then we use the constrained parameter spaces to predict the NP effects on other quantities, which have not been measured or have not been well measured yet. Section VI contains our summary and conclusion.

II. THE EXCLUSIVE $b \to u\ell^- \bar{\nu}_\ell$ DECAYS IN THE MSSM WITH AND WITHOUT R-PARITY VIOLATION

In supersymmetric extensions of the SM, there are gauge invariant interactions which violate the B and the L in general. To prevent occurrences of these B and L violating interactions in supersymmetric extensions of the SM, the additional global symmetry is required. This requirement leads to the consideration of the so-called R_p conservation (RPC).

*cskim@yonsei.ac.kr
†ruminwang@cskim.yonsei.ac.kr

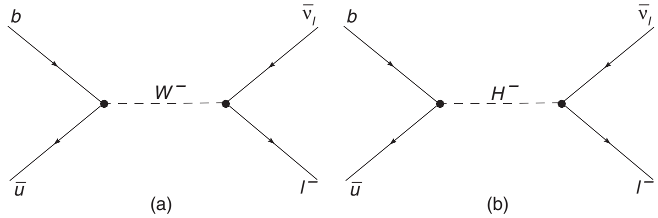

FIG. 1. The decays $b \to u\ell^- \bar{\nu}_\ell$ are mediated by a W boson exchange in the SM, and in extensions of the SM also by a charged Higgs exchange.

In the MSSM with RPC, the terms in the effective Hamiltonian relevant for the $b \to u\ell^- \bar{\nu}_\ell$ decays are

$$\mathcal{H}^{R_p}_{\rm eff}(b \to u\ell^- \bar{\nu}_\ell) = \frac{G_F}{\sqrt{2}} V_{ub}[(\bar{u}\gamma_\mu(1-\gamma_5)b) \times (\bar{\ell}\gamma^\mu(1-\gamma_5)\nu_\ell) - R_l(\bar{u}(1+\gamma_5)b) \times (\bar{\ell}(1-\gamma_5)\nu_\ell)], \quad (1)$$

here $R_l = \frac{\tan^2\beta}{m_H^2} \frac{\bar{m}_b m_l}{1+\epsilon_0 \tan\beta}$, parameter ϵ_0 is generated at the one-loop level (with the main contribution originating from gluino diagrams). Note that $\tilde{\epsilon}_0$ of [11] corresponds to ϵ_0 in our convention. The first term in Eq. (1) gives the SM contribution shown in Fig. 1(a), and the second one gives that of the charged Higgs scalars shown in Fig. 1(b).

Even though the requirement of RPC makes a theory consistent with present experimental searches, there is no good theoretical justification for this requirement. Therefore, the most general models with explicit R_p violation should be also considered. In the most general superpotential of the MSSM, the RPV superpotential is given by [21]

$$\mathcal{W}_{\not{R}_p} = \mu_i \hat{L}_i \hat{H}_u + \tfrac{1}{2}\lambda_{[ij]k} \hat{L}_i \hat{L}_j \hat{E}^c_k + \lambda'_{ijk} \hat{L}_i \hat{Q}_j \hat{D}^c_k + \tfrac{1}{2}\lambda''_{i[jk]} \hat{U}^c_i \hat{D}^c_j \hat{D}^c_k, \quad (2)$$

where $\hat{L}$ and $\hat{Q}$ are the SU(2) doublet lepton and quark superfields, respectively, $\hat{E}^c$, $\hat{U}^c$, and $\hat{D}^c$ are the singlet superfields, while i, j, and k are generation indices, and the superscript c denotes a charge conjugate field.

From Eq. (2), we can obtain the relevant four fermion effective Hamiltonian for the $b \to u_j \ell^-_m \bar{\nu}_{\ell n}$ processes with RPV couplings due to the squarks and sleptons exchange

$$\mathcal{H}_{\rm eff}(b \to u_j \ell^-_m \bar{\nu}_{\ell n})^{\not{R}_p} = -\sum_i \frac{\lambda'_{n3i}\lambda'^*_{mji}}{8m^2_{\tilde{d}_{iR}}}(\bar{u}_j\gamma_\mu(1-\gamma_5)b) \times (\bar{\ell}_m\gamma^\mu(1-\gamma_5)\nu_{\ell n}) + \sum_i \frac{\lambda_{inm}\lambda'^*_{ij3}}{4m^2_{\tilde{\ell}_{iL}}}(\bar{u}_j(1+\gamma_5)b) \times (\bar{\ell}_m(1-\gamma_5)\nu_{\ell n}). \quad (3)$$

The corresponding RPV Feynman diagrams for the $b \to u_j \ell^-_m \bar{\nu}_{\ell n}$ processes are displayed in Fig. 2. Note that the operators in Eq. (3) take the same form as those of the MSSM with RPC shown in Eq. (1).

Then, we can obtain the total effective Hamiltonian for the $b \to u\ell^- \bar{\nu}_\ell$ processes in the RPV MSSM

$$\begin{aligned}\mathcal{H}^{\not{R}_p}_{\rm eff}(b \to u\ell^- \bar{\nu}_\ell) &\equiv \mathcal{H}_{\rm eff}(b \to u\ell^- \bar{\nu}_\ell)^{\rm SM} + \mathcal{H}_{\rm eff}(b \to u\ell^- \bar{\nu}_\ell)^{\not{R}_p} \\ &= \left(\frac{G_F}{\sqrt{2}}V_{ub} - \sum_i \frac{\lambda'_{n3i}\lambda'^*_{mji}}{8m^2_{\tilde{d}_{iR}}}\right)(\bar{u}_j\gamma_\mu(1-\gamma_5)b)(\bar{\ell}_m\gamma^\mu(1-\gamma_5)\nu_{\ell n}) \\ &\quad + \sum_i \frac{\lambda_{inm}\lambda'^*_{ij3}}{4m^2_{\tilde{\ell}_{iL}}}(\bar{u}_j(1+\gamma_5)b)(\bar{\ell}_m(1-\gamma_5)\nu_{\ell n}). \end{aligned} \quad (4)$$

Note that the most general effective Hamiltonian of the RPV MSSM for the $b \to u\ell^- \bar{\nu}_\ell$ processes includes the SM part, the charged Higgs exchange part of RPC and the RPV sparticle exchange part. Because we do not want to take into account interferences between the charged Higgs exchanges and the RPV terms for the numerical purposes, we simply ignore the charged Higgs exchange part in $\mathcal{H}^{\not{R}_p}_{\rm eff}$.

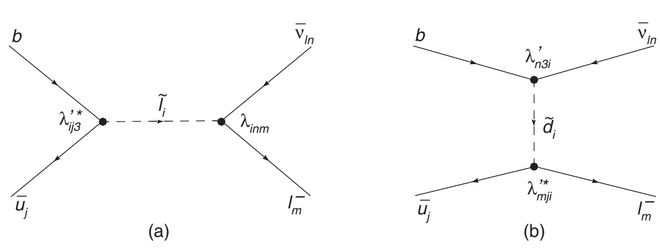

FIG. 2. The RPV contributions to the exclusive $b \to u_j \ell^-_m \bar{\nu}_{\ell n}$ decays due to sleptons and squarks exchange.

Based on the effective Hamiltonian in Eq. (4), we will give the expressions of physical quantities for the RPV MSSM later in detail. Note that the operators in Eq. (4) have exactly the same form as those of the MSSM with RPC shown in Eq. (1). For the expressions of the charged Higgs contributions, we just need let $\sum_i \frac{\lambda'_{n3i}\lambda'^*_{mji}}{8m^2_{\tilde{d}_{iR}}} = 0$ and replace $\sum_i \frac{\lambda_{inm}\lambda'^*_{ij3}}{4m^2_{\tilde{\ell}_{iL}}}$ with $-\frac{G_F}{\sqrt{2}}V_{ub}R_l$. In the following expressions and numerical analysis, we will keep the masses of all three generation charged leptons, but ignore all neutrino masses.

A. The branching ratio for $B_u^- \to \ell^- \bar{\nu}_\ell$

$B_u^- \to \ell^- \bar{\nu}_\ell$ decay amplitude can be obtained in terms of Eq. (4),

$$\begin{aligned}\mathcal{M}^{\not R_p}(B_u^- \to \ell^- \bar{\nu}_\ell) &= \langle \ell^- \bar{\nu}_\ell | \mathcal{H}_{\rm eff}^{\not R_p}(b \to u \ell^- \bar{\nu}_\ell) | B^- \rangle \\ &= \left[\frac{G_F}{\sqrt{2}} V_{ub} - \sum_i \frac{\lambda'_{n3i}\lambda'^*_{m1i}}{8m^2_{\tilde{d}_{iR}}} \right] \\ &\quad \times \langle 0 | \bar{u}\gamma_\mu(1-\gamma_5) b | B^- \rangle \\ &\quad \times \bar{\ell}_m \gamma^\mu (1-\gamma_5)\nu_{\ell n} + \sum_i \frac{\lambda_{inm}\lambda'^*_{i13}}{4m^2_{\tilde{\ell}_{iL}}} \\ &\quad \times \langle 0 | \bar{u}(1+\gamma_5) b | B^- \rangle \bar{\ell}_m (1-\gamma_5)\nu_{\ell n}. \end{aligned} \tag{5}$$

After using the definitions of the B meson decay constant [22]

$$\langle 0 | \bar{u}\gamma_\mu\gamma_5 b | B^- \rangle = i f_{B_u} p_{B\mu}, \tag{6}$$

$$\text{and} \quad \langle 0 | \bar{u}\gamma_5 b | B^- \rangle = -i f_{B_u}\mu_{B_u} \\ \text{with} \quad \mu_{B_u} \equiv \frac{m^2_{B_u}}{\bar{m}_b + \bar{m}_u}, \tag{7}$$

we get the branching ratio for $B_u^- \to \ell^- \bar{\nu}_\ell$

$$\begin{aligned}\mathcal{B}^{\not R_p}(B_u^- \to \ell^- \bar{\nu}_\ell) = &\left| \frac{G_F}{\sqrt{2}} V_{ub} - \sum_i \frac{\lambda'_{n3i}\lambda'^*_{m1i}}{8m^2_{\tilde{d}_{iR}}} \right. \\ &\left. + \sum_i \frac{\lambda_{inm}\lambda'^*_{i13}}{4m^2_{\tilde{\ell}_{iL}}} \frac{\mu_{B_u}}{m_\ell} \right|^2 \\ &\times \frac{\tau_{B_u}}{4\pi} f^2_{B_u} m_{B_u} m^2_\ell \left[1 - \frac{m^2_\ell}{m^2_{B_u}} \right]^2. \end{aligned} \tag{8}$$

From the above expression, we note that, unlike the contributions of squark exchange coupling $\lambda'_{n3i}\lambda'^*_{m1i}$ and the SM to $\mathcal{B}(B_u^- \to \ell^- \bar{\nu}_\ell)$, slepton exchange coupling $\lambda_{inm}\lambda'^*_{i13}$ is not suppressed by m^2_ℓ.

B. The branching ratio for $B_{(s)} \to P \ell^- \bar{\nu}_\ell (P = \pi, K)$

$B \to P\ell^- \bar{\nu}_\ell$ decay amplitude can be written as

$$\begin{aligned}\mathcal{M}^{\not R_p}(B \to P\ell^- \bar{\nu}_\ell) &= \langle P\ell^- \bar{\nu}_\ell | \mathcal{H}_{\rm eff}^{\not R_p}(b \to u \ell^- \bar{\nu}_\ell) | B \rangle \\ &= \left[\frac{G_F}{\sqrt{2}} V_{ub} - \sum_i \frac{\lambda'_{n3i}\lambda'^*_{m1i}}{8m^2_{\tilde{d}_{iR}}} \right] \\ &\quad \times \langle P | \bar{u}\gamma_\mu(1-\gamma_5) b | B \rangle \\ &\quad \times \bar{\ell}_m \gamma^\mu (1-\gamma_5)\nu_{\ell n} \\ &\quad + \sum_i \frac{\lambda_{inm}\lambda'^*_{i13}}{4m^2_{\tilde{\ell}_{iL}}} \langle P | \bar{u}(1+\gamma_5) b | B \rangle \\ &\quad \times \bar{\ell}_m (1-\gamma_5)\nu_{\ell n}. \end{aligned} \tag{9}$$

Using the $B \to P$ transition form factors [22]

$$\begin{aligned} c_P\langle P(p) | \bar{u}\gamma_\mu b | B(p_B) \rangle &= f_+^P(s)(p+p_B)_\mu \\ &\quad + [f_0^P(s) - f_+^P(s)] \frac{m_B^2 - m_P^2}{s} q_\mu, \end{aligned} \tag{10}$$

$$c_P\langle P(p) | \bar{u} b | B(p_B) \rangle = f_0^P(s) \frac{m_B^2 - m_P^2}{\bar{m}_b - \bar{m}_u}, \tag{11}$$

where the factor c_P accounts for the flavor content of particles ($c_P = \sqrt{2}$ for π^0, and $c_P = 1$ for π^-, K^-) and $s = q^2 (q = p_B - p)$, the differential branching ratio for $B \to P\ell^- \bar{\nu}_\ell$ is

$$\begin{aligned}\frac{d\mathcal{B}^{\not R_p}(B \to P\ell^- \bar{\nu}_\ell)}{ds d\cos\theta} &= \frac{\tau_B \sqrt{\lambda_P}}{2^7 \pi^3 m_B^3 c_P^2} \left(1 - \frac{m_\ell^2}{s} \right)^2 \\ &\quad \times [N_0^P + N_1^P \cos\theta + N_2^P \cos^2\theta], \end{aligned} \tag{12}$$

$$\begin{aligned} N_0^P = &\left| \frac{G_F}{\sqrt{2}} V_{ub} - \sum_i \frac{\lambda'_{n3i}\lambda'^*_{m1i}}{8m^2_{\tilde{d}_{iR}}} \right|^2 [f_+^P(s)]^2 \lambda_P \\ &+ \left| \frac{G_F}{\sqrt{2}} V_{ub} - \sum_i \frac{\lambda'_{n3i}\lambda'^*_{m1i}}{8m^2_{\tilde{d}_{iR}}} + \sum_i \frac{\lambda_{inm}\lambda'^*_{i13}}{4m^2_{\tilde{\ell}_{iL}}} \right. \\ &\left. \times \frac{s}{m_\ell(\bar{m}_b - \bar{m}_u)} \right|^2 m_\ell^2 [f_0^P(s)]^2 \frac{(m_B^2 - m_P^2)^2}{s}, \end{aligned} \tag{13}$$

$$\begin{aligned} N_1^P = &\left\{ \left| \frac{G_F}{\sqrt{2}} V_{ub} - \sum_i \frac{\lambda'_{n3i}\lambda'^*_{m1i}}{8m^2_{\tilde{d}_{iR}}} \right|^2 \right. \\ &+ \mathrm{Re}\left[\left(\frac{G_F}{\sqrt{2}} V_{ub} - \sum_i \frac{\lambda'_{n3i}\lambda'^*_{m1i}}{8m^2_{\tilde{d}_{iR}}} \right)^\dagger \sum_i \frac{\lambda_{inm}\lambda'^*_{i13}}{4m^2_{\tilde{\ell}_{iL}}} \right. \\ &\left.\left. \times \frac{s}{m_\ell(\bar{m}_b - \bar{m}_u)} \right] \right\} 2m_\ell^2 f_0^P(s) f_+^P(s) \sqrt{\lambda_P} \frac{(m_B^2 - m_P^2)}{s}, \end{aligned} \tag{14}$$

$$N_2^P = - \left| \frac{G_F}{\sqrt{2}} V_{ub} - \sum_i \frac{\lambda'_{n3i}\lambda'^*_{m1i}}{8m^2_{\tilde{d}_{iR}}} \right|^2 [f_+^P(s)]^2 \lambda_P \left(1 - \frac{m_\ell^2}{s} \right), \tag{15}$$

where θ is the angle between the momentum of the B meson and the charged lepton in the c.m. system of ℓ–ν, and the kinematic factor $\lambda_P = m_B^4 + m_P^4 + s^2 - 2m_B^2 m_P^2 - 2m_B^2 s - 2m_P^2 s$.

Here, we give the definition of the normalized forward-backward (FB) asymmetry of the charged lepton [23], which is more useful from the experimental point of view,

$$\bar{\mathcal{A}}_{\rm FB} = \frac{\int_0^{+1} \frac{d^2\mathcal{B}}{ds d\cos\theta} d\cos\theta - \int_{-1}^0 \frac{d^2\mathcal{B}}{ds d\cos\theta} d\cos\theta}{\int_0^{+1} \frac{d^2\mathcal{B}}{ds d\cos\theta} d\cos\theta + \int_{-1}^0 \frac{d^2\mathcal{B}}{ds d\cos\theta} d\cos\theta}. \tag{16}$$

Explicitly, for $B \to P\ell^- \bar{\nu}_\ell$ the normalized FB asymmetry is

$$\bar{\mathcal{A}}_{\rm FB}(B \to P\ell^-\bar{\nu}_\ell) = \frac{N_1^P}{2N_0^P + 2/3N_2^P}. \tag{17}$$

C. The branching ratio for $B_{(s)} \to V\ell^-\bar{\nu}_\ell (V = \rho, K^*)$

Similarly, the expression for $B \to V\ell^-\bar{\nu}_\ell$ decay amplitude is

$$\begin{aligned}\mathcal{M}^{\not R_p}(B \to V\ell^-\bar{\nu}_\ell) &= \langle V\ell^-\bar{\nu}_\ell|\mathcal{H}_{\rm eff}^{\not R_p}(b \to u\ell^-\bar{\nu}_\ell)|B\rangle \\ &= \Bigg[\frac{G_F}{\sqrt{2}}V_{ub} - \sum_i \frac{\lambda'_{n3i}\lambda'^*_{m1i}}{8m^2_{\tilde{d}_{iR}}}\Bigg] \\ &\quad\times \langle V|\bar{u}\gamma_\mu(1-\gamma_5)b|B\rangle\bar{\ell}_m \\ &\quad\times \gamma^\mu(1-\gamma_5)\nu_{\ell n} + \sum_i \frac{\lambda_{inm}\lambda'^*_{i13}}{4m^2_{\tilde{\ell}_{iL}}} \\ &\quad\times \langle V|\bar{u}(1+\gamma_5)b|B\rangle\bar{\ell}_m(1-\gamma_5)\nu_{\ell n}.\end{aligned} \tag{18}$$

In terms of the $B \to V$ form factors [22]

$$\begin{aligned}c_V\langle V(p,\varepsilon^*)|\bar{u}\gamma_\mu(1-\gamma_5)b|B(p_B)\rangle &= \frac{2V^V(s)}{m_B+m_V}\epsilon_{\mu\nu\alpha\beta}\varepsilon^{*\nu}p_B^\alpha p^\beta \\ &\quad - i\Bigg[\varepsilon^*_\mu(m_B+m_V)A_1^V(s) \\ &\quad - (p_B+p)_\mu(\varepsilon^*\cdot p_B)\frac{A_2^V(s)}{m_B+m_V}\Bigg] \\ &\quad + iq_\mu(\varepsilon^*\cdot p_B)\frac{2m_V}{s}[A_3^V(s) - A_0^V(s)],\end{aligned} \tag{19}$$

$$c_V\langle V(p,\varepsilon^*)|\bar{u}\gamma_5 b|B(p_B)\rangle = -i\frac{\varepsilon^*\cdot p_B}{m_B}\frac{2m_Bm_V}{\bar{m}_b+\bar{m}_u}A_0^V(s), \tag{20}$$

where $c_V = \sqrt{2}$ for ρ^0, $c_V = 1$ for ρ^-, K^{*-} and with the relation $A_3^V(s) = \frac{m_B+m_V}{2m_V}A_1^V(s) - \frac{m_B-m_V}{2m_V}A_2^V(s)$, we have

$$\frac{d\mathcal{B}^{\not R_p}(B \to V\ell^-\bar{\nu}_\ell)}{ds\,d\cos\theta} = \frac{\tau_B\sqrt{\lambda_V}}{2^7\pi^3m_B^3c_V^2}\left(1-\frac{m_\ell^2}{s}\right)^2 \times [N_0^V + N_1^V\cos\theta + N_2^V\cos^2\theta], \tag{21}$$

$$\begin{aligned}N_0^V = {}& \Bigg|\frac{G_F}{\sqrt{2}}V_{ub} - \sum_i\frac{\lambda'_{n3i}\lambda'^*_{m1i}}{8m^2_{\tilde{d}_{iR}}}\Bigg|^2\Bigg\{[A_1^V(s)]^2\bigg(\frac{\lambda_V}{4m_V^2} + (m_\ell^2+2s)\bigg)(m_B+m_V)^2 + [A_2^V(s)]^2\frac{\lambda_V^2}{4m_V^2(m_B+m_V)^2} \\ &+ [V^V(s)]^2\frac{\lambda_V}{(m_B+m_V)^2}(m_\ell^2+s) - A_1^V(s)A_2^V(s)\frac{\lambda_V}{2m_V^2}(m_B^2-s-m_V^2)\Bigg\} \\ &+ \Bigg|\frac{G_F}{\sqrt{2}}V_{ub} - \sum_i\frac{\lambda'_{n3i}\lambda'^*_{m1i}}{8m^2_{\tilde{d}_{iR}}} + \sum_i\frac{\lambda_{inm}\lambda'^*_{i13}}{4m^2_{\tilde{\ell}_{iL}}}\frac{s}{m_\ell(\bar{m}_b+\bar{m}_u)}\Bigg|^2[A_0^V(s)]^2\frac{m_\ell^2}{s}\lambda_V,\end{aligned} \tag{22}$$

$$\begin{aligned}N_1^V = {}& \Bigg\{\Bigg|\frac{G_F}{\sqrt{2}}V_{ub} - \sum_i\frac{\lambda'_{n3i}\lambda'^*_{m1i}}{8m^2_{\tilde{d}_{iR}}}\Bigg|^2 + \mathrm{Re}\Bigg[\bigg(\frac{G_F}{\sqrt{2}}V_{ub} - \sum_i\frac{\lambda'_{n3i}\lambda'^*_{m1i}}{8m^2_{\tilde{d}_{iR}}}\bigg)^\dagger\sum_i\frac{\lambda_{inm}\lambda'^*_{i13}}{4m^2_{\tilde{\ell}_{iL}}}\frac{s}{m_\ell(\bar{m}_b+\bar{m}_u)}\Bigg]\Bigg\} \\ &\times\Bigg[A_0^V(s)A_1^V(s)\frac{m_\ell^2(m_B+m_V)(m_B^2-m_V^2-s)\sqrt{\lambda_V}}{sm_V} - A_0^V(s)A_2^V(s)\frac{m_\ell^2\lambda_V^{3/2}}{sm_V(m_B+m_V)}\Bigg] \\ &+ \Bigg|\frac{G_F}{\sqrt{2}}V_{ub} - \sum_i\frac{\lambda'_{n3i}\lambda'^*_{m1i}}{8m^2_{\tilde{d}_{iR}}}\Bigg|^2 A_1^V(s)V^V(s)4s\sqrt{\lambda_V},\end{aligned} \tag{23}$$

$$\begin{aligned}N_2^V = {}& -\Bigg|\frac{G_F}{\sqrt{2}}V_{ub} - \sum_i\frac{\lambda'_{n3i}\lambda'^*_{m1i}}{8m^2_{\tilde{d}_{iR}}}\Bigg|^2\bigg(1-\frac{m_\ell^2}{s}\bigg)\lambda_V\Bigg\{[A_1^V(s)]^2\frac{(m_B+m_V)^2}{4m_V^2} + [V^V(s)]^2\frac{s}{(m_B+m_V)^2} \\ &+ [A_2^V(s)]^2\frac{\lambda_V}{4m_V^2(m_B+m_V)^2} - A_1^V(s)A_2^V(s)\frac{m_B^2-m_V^2-s}{2m_V^2}\Bigg\},\end{aligned} \tag{24}$$

where $\lambda_V = m_B^4 + m_V^4 + s^2 - 2m_B^2m_V^2 - 2m_B^2s - 2m_V^2s$.

From Eq. (16), the normalized FB asymmetry of $B \to V\ell^-\bar{\nu}_\ell$ can be written as

$$\bar{\mathcal{A}}_{\rm FB}(B \to V\ell^-\bar{\nu}_\ell) = \frac{N_1^V}{2N_0^V + 2/3N_2^V}. \tag{25}$$

For $B \to V\ell^-\bar{\nu}_\ell$ decay, besides the branching ratio and the normalized FB asymmetry of the charged lepton, another interesting observable is the ratio of longitudinal to transverse polarization of the vector meson Γ_L^V/Γ_T^V, which can be derived from the following differential expressions

$$\frac{d\Gamma_L^{\not R_p}}{ds} = \frac{\sqrt{\lambda_V}}{2^7\pi^3 m_B^3 c_V^2}\left(1-\frac{m_\ell^2}{s}\right)^2\left\{\left|\frac{G_F}{\sqrt{2}}V_{ub} - \sum_i \frac{\lambda'_{n3i}\lambda'^*_{m1i}}{8m^2_{\tilde{d}_{iR}}}\right|^2\left(\frac{4}{3}+\frac{2m_\ell^2}{3s}\right)\left([A_1^V(s)]^2\frac{(m_B^2-m_V^2-s)^2(m_B+m_V)^2}{4m_V^2}\right.\right.$$
$$\left. + [A_2^V(s)]^2\frac{\lambda_V^2}{4m_V^2(m_B+m_V)^2} - A_1^V(s)A_2^V(s)\frac{(m_B^2-m_V^2-s)\lambda_V}{4m_V^2}\right)$$
$$\left. + 2\left|\frac{G_F}{\sqrt{2}}V_{ub} - \sum_i \frac{\lambda'_{n3i}\lambda'^*_{m1i}}{8m^2_{\tilde{d}_{iR}}} + \sum_i \frac{\lambda_{inm}\lambda'^*_{i13}}{4m^2_{\tilde{\ell}_{iL}}}\frac{s}{m_\ell(\bar{m}_b+\bar{m}_u)}\right|^2[A_0^V(s)]^2\frac{m_\ell^2}{s}\lambda_V\right\}, \tag{26}$$

$$\frac{d\Gamma_T^{\not R_p}}{ds} = \frac{\sqrt{\lambda_V}}{2^7\pi^3 m_B^3 c_V^2}\left(1-\frac{m_\ell^2}{s}\right)^2\left|\frac{G_F}{\sqrt{2}}V_{ub} - \sum_i \frac{\lambda'_{n3i}\lambda'^*_{m1i}}{8m^2_{\tilde{d}_{iR}}}\right|^2\frac{8}{3}\left\{[A_1^V(s)]^2(m_\ell^2+2s)(m_B+m_V)^2 + [V^V(s)]^2\frac{\lambda_V(m_\ell^2+2s)}{(m_B+m_V)^2}\right\}. \tag{27}$$

In this section, we give the expressions of only the exclusive $b \to u\ell^-\bar{\nu}_\ell$ decays, but we will use the CP averaged results of the exclusive $b \to u\ell^-\bar{\nu}_\ell$ and $\bar{b} \to \bar{u}\ell^+\nu_\ell$ decays in our numerical analysis.

III. INPUT PARAMETERS

The input parameters except the form factors are collected in Table I. In our numerical results, we will use the input parameters, which are varied randomly within 1σ range.

For the form factors involving the $B \to P(V)$ transitions, we will use the recent light-cone QCD sum rule results [22], which are renewed with radiative corrections to the leading twist wave functions and SU(3) breaking effects. For the s-dependence of the form factors, they can be parameterized in terms of simple formulae with two or three parameters. The form factors V^V, A_0^V, and f_+^π are parameterized by

$$F(s) = \frac{r_1}{1-s/m_R^2} + \frac{r_2}{1-s/m_{\rm fit}^2}. \tag{28}$$

For the form factors A_2^V and f_+^K, it is more appropriate to expand to second order around the pole, yielding

$$F(s) = \frac{r_1}{1-s/m^2} + \frac{r_2}{(1-s/m^2)^2}, \tag{29}$$

where $m = m_{\rm fit}$ for A_2^V and $m = m_R$ for f_+^K. The fit formula for A_1^V and f_0^P is

$$F(s) = \frac{r_2}{1-s/m_{\rm fit}^2}. \tag{30}$$

However, $B_s \to K$ form factors are not given in recent light-cone QCD sum rule results [22]. After discussions with authors of Ref. [22], we obtain them as

$$F^{B_s\to K}(s) = F^{B_{u,d}\to K}(s)\left(\frac{F^{B_s\to K^*}(s)}{F^{B_{u,d}\to K^*}(s)}\right). \tag{31}$$

All the corresponding parameters for these form factors are collected in Table II.

We have several remarks on the input parameters:

(i) *Form factor*: The uncertainties of form factors at $s = 0$ induced by $F(0)$ are considered.

(ii) *CKM matrix element*: Using experimental measurements of $|V_{ub}|$ from the inclusive $b \to u$ semileptonic B decays, these exclusive $b \to u\ell^-\bar{\nu}_\ell$ decays can be used to constrain the parameters of theories beyond the SM. The weak phase γ is well constrained in the SM; however, with the presence of R_p violation, this constraint may be relaxed. We will not take γ within the SM range, but vary it randomly in the range of 0 to π to obtain conservative limits on RPV coupling products.

(iii) *RPV coupling*: When we study the RPV effects, we consider only one RPV coupling product contributes at one time, neglecting the interferences between different RPV coupling products, but keeping their interferences with the SM amplitude. We assume the masses of sfermion are 100 GeV. For other values of

TABLE I. Default values of the input parameters and the $\pm 1\sigma$ error ranges for the sensitive parameters used in our numerical calculations.

$m_{B_s} = 5.366$ GeV, $m_{B_d} = 5.279$ GeV, $m_{B_u} = 5.279$ GeV, $m_{K^{*\pm}} = 0.892$ GeV, $m_{\pi^\pm} = 0.140$ GeV, $m_{\pi^0} = 0.135$ GeV, $m_\rho = 0.775$ GeV, $m_{K^\pm} = 0.494$ GeV, $\bar{m}_b(\bar{m}_b) = (4.20 \pm 0.07)$ GeV, $\bar{m}_u(2\text{ GeV}) = 0.0015 \sim 0.003$ GeV, $m_e = 0.511\times10^{-3}$ GeV, $m_\mu = 0.106$ GeV, $m_\tau = 1.777$ GeV	[24]
$\tau_{B_s} = (1.437^{+0.030}_{-0.031})$ ps, $\tau_{B_d} = (1.530 \pm 0.009)$ ps, $\tau_{B_u} = (1.638 \pm 0.011)$ ps.	[24]
$f_{B_u} = 0.161 \pm 0.013$ GeV	[22]
$\lvert V_{ub}\rvert = (4.31 \pm 0.39)\times10^{-3}$	[25]
$\epsilon_0 \in [-0.01, 0.01]$	[11]

TABLE II. Fit for form factors involving the $B \to K^{(*)}$ and $B \to \rho(\pi)$ transitions valid for general s [22].

$F(s)$	$F(0)$	r_1	m_R^2	r_2	$m_{\rm fit}^2$	Fit Equation
$V^{B_{u,d}\to\rho}$	0.323 ± 0.030	1.045	5.32^2	-0.721	38.34	(28)
$A_0^{B_{u,d}\to\rho}$	0.303 ± 0.029	1.527	5.28^2	-1.220	33.36	(28)
$A_1^{B_{u,d}\to\rho}$	0.242 ± 0.023			0.240	37.51	(30)
$A_2^{B_{u,d}\to\rho}$	0.221 ± 0.023	0.009		0.212	40.82	(29)
$V^{B_{u,d}\to K^*}$	0.411 ± 0.033	0.923	5.32^2	-0.511	49.40	(28)
$A_0^{B_{u,d}\to K^*}$	0.374 ± 0.033	1.364	5.28^2	-0.990	36.78	(28)
$A_1^{B_{u,d}\to K^*}$	0.292 ± 0.028			0.290	40.38	(30)
$A_2^{B_{u,d}\to K^*}$	0.259 ± 0.027	-0.084		0.342	52.00	(29)
$V^{B_s\to K^*}$	0.311 ± 0.026	2.351	5.42^2	-2.039	33.10	(28)
$A_0^{B_s\to K^*}$	0.360 ± 0.034	2.813	5.37^2	-2.509	31.58	(28)
$A_1^{B_s\to K^*}$	0.233 ± 0.022			0.231	32.94	(30)
$A_2^{B_s\to K^*}$	0.181 ± 0.025	-0.011		0.192	40.14	(29)
$f_+^{B_{u,d}\to\pi}$	0.258 ± 0.031	0.744	5.32^2	-0.486	40.73	(28)
$f_0^{B_{u,d}\to\pi}$	0.258 ± 0.031	0		0.258	33.81	(30)
$f_+^{B_{u,d}\to K}$	0.331 ± 0.041	0.162	5.41^2	0.173		(29)
$f_0^{B_{u,d}\to K}$	0.331 ± 0.041	0		0.331	37.46	(30)

the sfermion masses, the bounds on the couplings in this paper can be easily obtained by scaling them by factor $\tilde{f}^2 \equiv (\frac{m_{\tilde{f}}}{100\ \mathrm{GeV}})^2$.

IV. NUMERICAL RESULTS IN THE MSSM WITH RPC

In this section, we study the charged Higgs contributions to the exclusive $\bar{b} \to \bar{u}\ell^+\nu_\ell$ decays in the MSSM with RPC. Since the couplings of the charged Higgs to the leptons are always proportional to the charged lepton masses (see the foregoing equations), it is easy to understand that the effects of the charged Higgs will not significantly affect in the case of the light leptonic decays, so we only present the charged Higgs contributions to the exclusive $\bar{b} \to \bar{u}\tau^+\nu_\tau$ decays. Based on the constraint of the charged Higgs effects from the measurement on $\mathcal{B}(B^+ \to \tau^+\nu_\tau)$, we investigate these effects on $\mathcal{B}$, $d\mathcal{B}/ds$, $\bar{\mathcal{A}}_{\rm FB}$, and Γ_L^V/Γ_T^V in the exclusive $\bar{b} \to \bar{u}\tau^+\nu_\tau$ semileptonic decays.

Note that the charged Higgs effects on the exclusive $\bar{b} \to \bar{u}\tau^+\nu_\tau$ decays have been discussed in Ref. [26], which fixed $\tan\beta = 50$ and let the physical quantity as a function of m_H. Here we will not choose $\tan\beta$ as a fixed value but let the observable as a function of $\tan\beta$ and m_H to study the effects of $\tan\beta$ and m_H. In addition, we will investigate the charged Higgs contributions to Γ_L^V/Γ_T^V, which has not been studied yet. For the exclusive $\bar{b} \to \bar{u}\tau^+\nu_\tau$ decays, the purely leptonic decay $B_u^+ \to \tau^+\nu_\tau$ has been measured by *BABAR* [27] and Belle [28]. We will use the averaged experimental data from Heavy Flavor Averaging Group [25]

$$\mathcal{B}(B_u^+ \to \tau^+\nu_\tau) = (1.41^{+0.43}_{-0.42}) \times 10^{-4}. \qquad (32)$$

Using the experimental data of $\mathcal{B}(B_u^+ \to \tau^+\nu_\tau)$ varied randomly within 1σ range and considering the theoretical uncertainties, we constrain the allowed range of $\tan\beta/m_H$, which is shown in Fig. 3(a). The corresponding bound from the upper limit of $\mathcal{B}(B_u^+ \to \mu^+\nu_\mu) < 1.7 \times 10^{-6}$ is also displayed in Fig. 3(b), in which the bound is weaker than

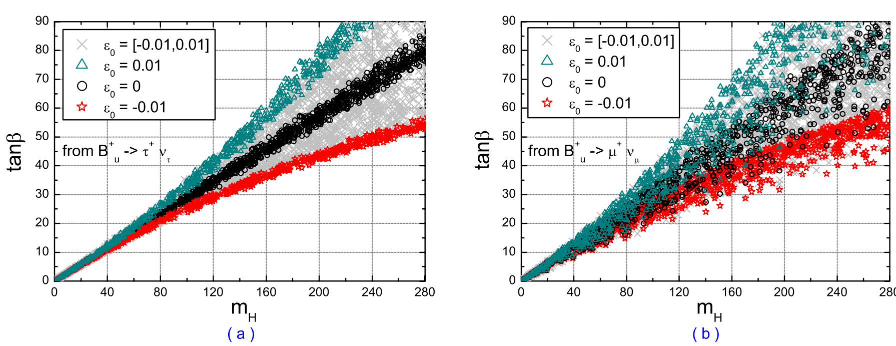

FIG. 3 (color online). The allowed regions in the $\tan\beta$-m_H plane for different values of ϵ_0. Plot (a) is constrained from the experimental data of $\mathcal{B}(B_u^+ \to \tau^+\nu_\tau)$, and plot (b) is constrained from the upper limit of $\mathcal{B}(B_u^+ \to \mu^+\nu_\mu)$.

TABLE III. The allowed ranges of $\tan\beta/m_H$ from $\mathcal{B}(B_u^+ \to \tau^+ \nu_\tau)$ and $\mathcal{B}(B_u^+ \to \mu^+ \nu_\mu)$.

		$\epsilon_0 = 0$	$\epsilon_0 \in [-0.01, 0.01]$
$\tan\beta/m_H$	from $\mathcal{B}(B_u^+ \to \tau^+ \nu_\tau)$	$[0.26, 0.31]$ GeV^{-1}	$[0.18, 0.49]$ GeV^{-1}
$\tan\beta/m_H$	from $\mathcal{B}(B_u^+ \to \mu^+ \nu_\mu)$	$[0.20, 0.34]$ GeV^{-1}	$[0.15, 0.57]$ GeV^{-1}

one from $\mathcal{B}(B_u^+ \to \tau^+ \nu_\tau)$. At present, the most stringent bound comes from $B_u^+ \to \tau^+ \nu_\tau$. The numerical ranges of $\tan\beta/m_H$ without the radiative corrections ($\epsilon_0 = 0$) and with inclusion of radiative corrections ($\epsilon_0 \in [-0.01, 0.01]$) are given in Table III. In Ref. [29], from the experimental upper limit of $\mathcal{B}(B_u^+ \to \tau^+ \nu_\tau) < 4.1 \times 10^{-4}$, the authors got $\tan\beta/m_H = 0.34(0.36, 0.32)$ GeV^{-1} for $f_{B_u} = 0.2(0.17, 0.23)$ GeV with $\epsilon_0 = 0$. Our bounds on $\tan\beta/m_H$, from new data of $\mathcal{B}(B_u^+ \to \tau^+ \nu_\tau)$ and considering all theoretical uncertainties, are much stronger than theirs, as shown in Table III.

Using the constrained $\tan\beta/m_H$ from $\mathcal{B}(B_u^+ \to \tau^+ \nu_\tau)$, one can predict the charged Higgs effects on the semileptonic decays $B_u^+ \to \pi^0 \tau^+ \nu_\tau$, $B_d^0 \to \pi^- \tau^+ \nu_\tau$, $B_s^0 \to K^- \tau^+ \nu_\tau$, $B_u^+ \to \rho^0 \tau^+ \nu_\tau$, $B_d^0 \to \rho^- \tau^+ \nu_\tau$, and $B_s^0 \to K^{*-} \tau^+ \nu_\tau$. With the expressions for $\mathcal{B}$ and Γ_L^V/Γ_T^V at hand, we perform a scan on the input parameters and the newly constrained $\tan\beta/m_H$. Then, the allowed ranges for $\mathcal{B}$ and Γ_L^V/Γ_T^V are obtained including the charged Higgs contributions, which satisfy present experimental constraint of $\mathcal{B}(B_u^+ \to \tau^+ \nu_\tau)$ shown in Eq. (32). Our numerical results are summarized in Table IV, in which we find that the charged Higgs contributions could slightly reduce $\mathcal{B}(B \to P(V)\tau\nu_\tau)$ and $\frac{\Gamma_L}{\Gamma_T}(B \to V \tau^+ \nu_\tau)$.

Now, we present correlations between the physical observables and the charged Higgs effects by the two-dimensional scatter plots, and moreover, we give the SM predictions for comparison. The charged Higgs effects on $B_u^+ \to \pi^0 \tau^+ \nu_\tau$, $B_d^0 \to \pi^- \tau^+ \nu_\tau$, and $B_s^0 \to K^- \tau^+ \nu_\tau$ are very similar to each other; therefore we will take $B_d^0 \to \pi^- \tau^+ \nu_\tau$ decay as an example. For the same reason, we will only display the charged Higgs effects on $B_d^0 \to \rho^- \tau^+ \nu_\tau$ among the other three decay modes $B_u^+ \to \rho^0 \tau^+ \nu_\tau$, $B_d^0 \to \rho^- \tau^+ \nu_\tau$, and $B_s^0 \to K^{*-} \tau^+ \nu_\tau$. The charged Higgs effects on $B_d^0 \to \pi^-(\rho^-)\tau^+ \nu_\tau$ decays are shown in Fig. 4.

TABLE IV. The theoretical predictions of the exclusive $\bar{b} \to \bar{u}\tau^+ \nu_\tau$ decays for $\mathcal{B}(\times 10^{-4})$ and Γ_L^V/Γ_T^V in the SM and in the MSSM with RPC.

	SM value	MSSM value with RPC
$\mathcal{B}(B_u^+ \to \pi^0 \tau^+ \nu_\tau)$	[0. 58, 1.22]	[0.43, 0.96]
$\mathcal{B}(B_d^0 \to \pi^- \tau^+ \nu_\tau)$	[1.12, 2.28]	[0.80, 1.79]
$\mathcal{B}(B_s^0 \to K^- \tau^+ \nu_\tau)$	[1.47, 3.05]	[1.02, 2.37]
$\mathcal{B}(B_u^+ \to \rho^0 \tau^+ \nu_\tau)$	[0.97, 2.19]	[0.83, 2.02]
$\mathcal{B}(B_d^0 \to \rho^- \tau^+ \nu_\tau)$	[1.83, 4.08]	[1.56, 3.78]
$\mathcal{B}(B_s^0 \to K^{*-} \tau^+ \nu_\tau)$	[2.08, 4.46]	[1.64, 4.06]
$\frac{\Gamma_L}{\Gamma_T}(B_u^+ \to \rho^0 \tau^+ \nu_\tau)$	[0.65, 1.19]	[0.45, 1.03]
$\frac{\Gamma_L}{\Gamma_T}(B_d^0 \to \rho^- \tau^+ \nu_\tau)$	[0.65, 1.19]	[0.45, 1.03]
$\frac{\Gamma_L}{\Gamma_T}(B_s^0 \to K^{*-} \tau^+ \nu_\tau)$	[0.84, 1.38]	[0.58, 1.11]

From Fig. 4(a)–4(c), we can see that $\mathcal{B}(B_d^0 \to \pi^- \tau^+ \nu_\tau)$, $\mathcal{B}(B_d^0 \to \rho^- \tau^+ \nu_\tau)$, and $\frac{\Gamma_L}{\Gamma_T}(B_d^0 \to \rho^- \tau^+ \nu_\tau)$ are not much sensitive to the change of $\tan\beta/m_H$, but the charged Higgs contributions can slightly reduce these quantities. As shown in Fig. 4(d)–4(g), the charged Higgs have also reducing effects on $d\mathcal{B}/ds$ and $\bar{\mathcal{A}}_{\mathrm{FB}}$. Especially, the sign of $\bar{\mathcal{A}}_{\mathrm{FB}}(B_d^0 \to \pi^- \tau^+ \nu_\tau)$ could be changed by the effect. According to Eqs. (12)–(17), since the normalized FB asymmetry of $B \to P \ell^+ \nu_\ell$ is associated with $m_\ell^2 f_0^P(s) f_+^P(s)$ and not suppressed by s, we can easily understand that $\bar{\mathcal{A}}_{\mathrm{FB}}(B_d^0 \to \pi^- \tau^+ \nu_\tau)$ shown in Fig. 4(f) could be significantly affected by the charged Higgs couplings. Therefore, $\bar{\mathcal{A}}_{\mathrm{FB}}(B \to P \tau^+ \nu_\tau)$ are very powerful quantities to be measured, to constrain the charged Higgs effects in the MSSM with RPC.

V. NUMERICAL RESULTS IN THE RPV MSSM

A. The exclusive $\bar{b} \to \bar{u}\tau^+ \nu_\tau$ decays

There are two RPV coupling products, $\lambda'^*_{33i}\lambda'_{31i}$ and $\lambda^*_{i33}\lambda'_{i13}$, contributing to seven exclusive $\bar{b} \to \bar{u}\tau^+ \nu_\tau$ decay modes, $B_u^+ \to \tau^+ \nu_\tau$, $B_u^+ \to \pi^0 \tau^+ \nu_\tau$, $B_d^0 \to \pi^- \tau^+ \nu_\tau$, $B_s^0 \to K^- \tau^+ \nu_\tau$, $B_u^+ \to \rho^0 \tau^+ \nu_\tau$, $B_d^0 \to \rho^- \tau^+ \nu_\tau$, and $B_s^0 \to K^{*-} \tau^+ \nu_\tau$. We use the experimental data of $\mathcal{B}(B_u^+ \to \tau^+ \nu_\tau)$, which is varied randomly within 1σ range to constrain the two RPV coupling products. Our bounds on the two RPV coupling products are demonstrated in Fig. 5, in which we find that every RPV weak phase is not much constrained, but the modulus of the relevant RPV coupling products can be tightly upper limited. The upper limits for the relevant RPV coupling products are summarized in Table V. Note that the bounds on the direct quadric couplings have not been estimated in previous $\bar{b} \to \bar{u}\tau^+ \nu_\tau$ studies. Our bounds on the RPV quadric couplings from $B_u^+ \to \tau^+ \nu_\tau$ are weaker than the bounds, which are calculated from the products of the smallest values of two single couplings in [30,31].

Using the constrained parameter spaces shown in Fig. 5, we will predict the RPV effects on other quantities which have not been measured yet in the exclusive $\bar{b} \to \bar{u}\tau^+ \nu_\tau$ decays. The allowed ranges for $\mathcal{B}$ and Γ_L^V/Γ_T^V are obtained with the different RPV coupling products, which are summarized in Table VI. We can find some salient features of the numerical results listed in Table VI.

(1) The contributions of $\lambda'^*_{33i}\lambda'_{31i}$ due to squark exchange will little enhance the branching ratios

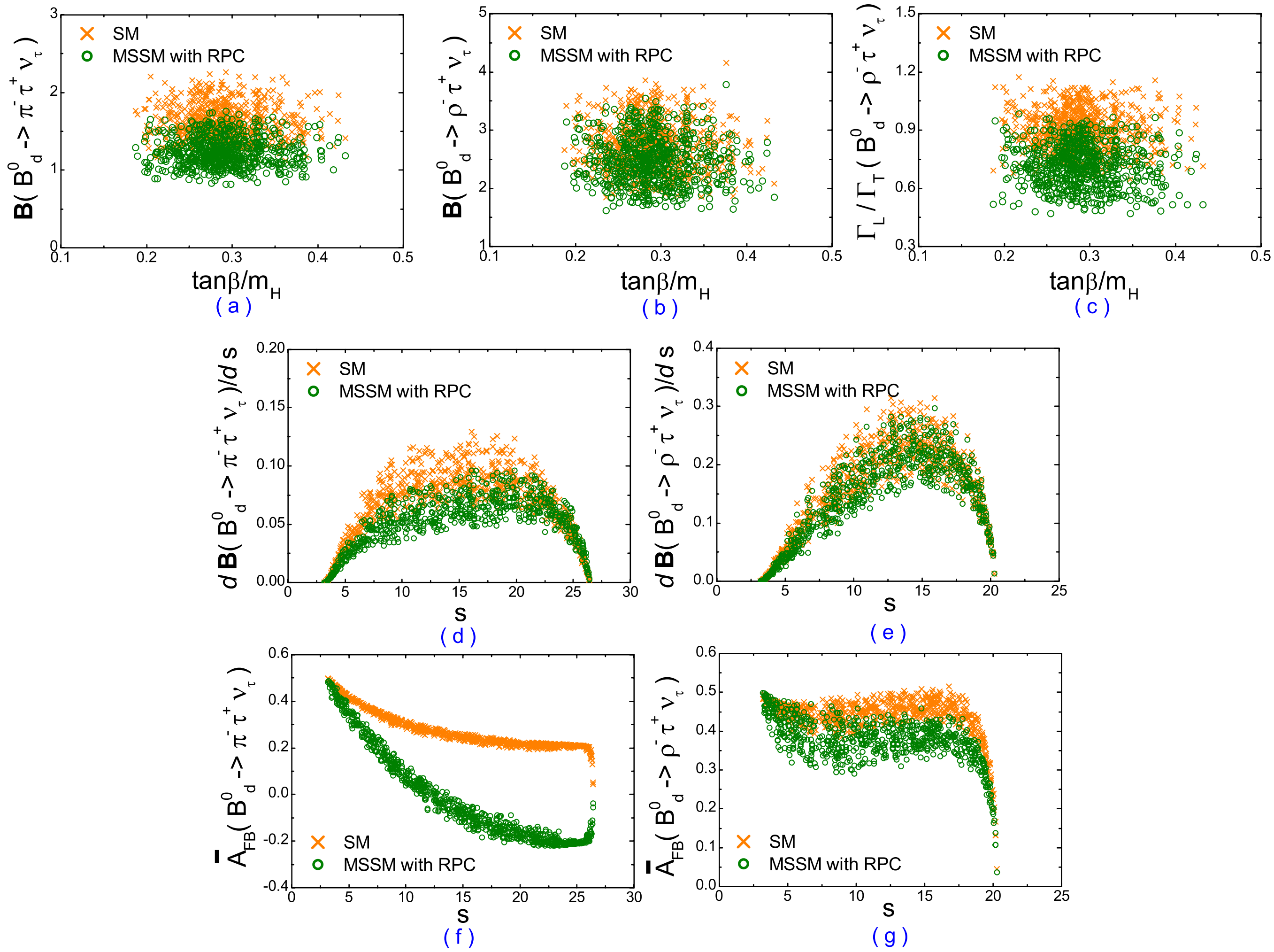

FIG. 4 (color online). The charged Higgs effects on $B_d^0 \to \pi^-(\rho^-)\tau^+\nu_\tau$ decays in the MSSM with RPC. $\mathcal{B}$ and $d\mathcal{B}/ds$ are in unit of 10^{-4}.

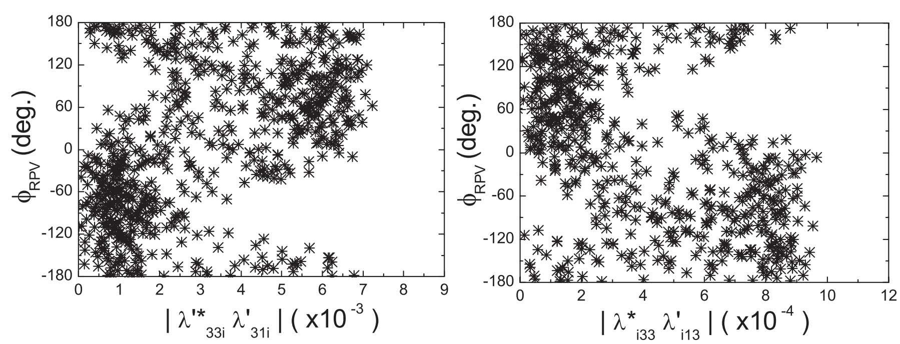

FIG. 5. The allowed parameter spaces for the relevant RPV coupling products constrained by the experimental data of $\mathcal{B}(B_u^+ \to \tau^+\nu_\tau)$.

$\mathcal{B}(B \to P\tau^+\nu_\tau)$ and $\mathcal{B}(B \to V\tau^+\nu_\tau)$. Because the effective Hamiltonian of squark exchange is proportional to operator $(\bar{b}\gamma_\mu(1-\gamma_5)u)(\bar{\nu}_\tau\gamma^\mu(1-\gamma_5)\tau)$, which is the same as the SM one, the effects of squark exchange are completely canceled in $\frac{\Gamma_L}{\Gamma_T}(B \to V\tau^+\nu_\tau)$.

TABLE V. Bounds for the relevant RPV coupling products by $B_u^+ \to \tau^+\nu_\tau$ decay for 100 GeV sfermions.

Couplings	Bounds [Processes]
$\lvert\lambda'^*_{33i}\lambda'_{31i}\rvert$	$\leq 7.28 \times 10^{-3}[B_u^+ \to \tau^+\nu_\tau]$
$\lvert\lambda^*_{i33}\lambda'_{i13}\rvert$	$\leq 9.65 \times 10^{-4}[B_u^+ \to \tau^+\nu_\tau]$

TABLE VI. The theoretical predictions of the exclusive $\bar{b} \to \bar{u}\tau^+\nu_\tau$ decays for $\mathcal{B}(\times 10^{-4})$ and Γ_L^V/Γ_T^V in the SM and the RPV MSSM. The RPV MSSM predictions are obtained by the constrained regions of the dierent RPV coupling products.

	SM value	MSSM value w/$\lambda'^*_{33i}\lambda'_{31i}$	MSSM value w/$\lambda^*_{i33}\lambda'_{i13}$
$\mathcal{B}(B_u^+ \to \pi^0\tau^+\nu_\tau)$	[0.58, 1.22]	[0.78, 2.47]	[0.49, 1.30]
$\mathcal{B}(B_d^0 \to \pi^-\tau^+\nu_\tau)$	[1.12, 2.28]	[1.45, 4.59]	[0.91, 2.41]
$\mathcal{B}(B_s^0 \to K^-\tau^+\nu_\tau)$	[1.47, 3.05]	[1.92, 5.91]	[1.18, 3.35]
$\mathcal{B}(B_u^+ \to \rho^0\tau^+\nu_\tau)$	[0.97, 2.19]	[1.42, 4.07]	[0.89, 2.17]
$\mathcal{B}(B_d^0 \to \rho^-\tau^+\nu_\tau)$	[1.83, 4.08]	[2.64, 7.57]	[1.65, 4.04]
$\mathcal{B}(B_s^0 \to K^{*-}\tau^+\nu_\tau)$	[2.08, 4.46]	[2.85, 9.62]	[1.96, 4.57]
$\frac{\Gamma_L}{\Gamma_T}(B_u^+ \to \rho^0\tau^+\nu_\tau)$	[0.65,1.19]	$\cdots$	[0.47,1.22]
$\frac{\Gamma_L}{\Gamma_T}(B_d^0 \to \rho^-\tau^+\nu_\tau)$	[0.65, 1.19]	$\cdots$	[0.47, 1.22]
$\frac{\Gamma_L}{\Gamma_T}(B_s^0 \to K^{*-}\tau^+\nu_\tau)$	[0.84, 1.38]	$\cdots$	[0.68, 1.41]

(2) As for the contributions of $\lambda^*_{i33}\lambda'_{i13}$ due to slepton exchange, the slepton exchange coupling has no obvious effects on $\mathcal{B}(B \to P(V)\tau^+\nu_\tau)$, but the allowed ranges of $\frac{\Gamma_L}{\Gamma_T}(B \to V\tau^+\nu_\tau)$ can be enlarged by this coupling, especially, their allowed lower limits are observably decreased.

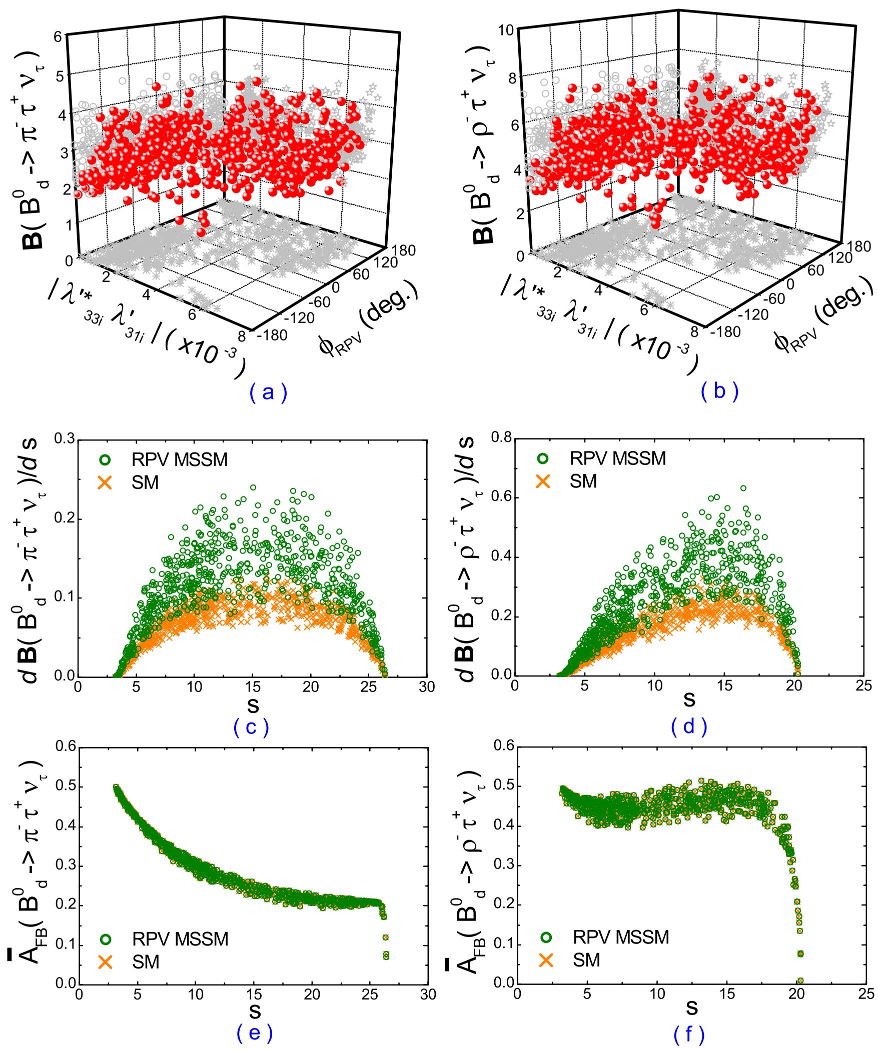

FIG. 6 (color online). The effects of RPV coupling $\lambda'^*_{33i}\lambda'_{31i}$ on $B_d^0 \to \pi^-(\rho^-)\tau^+\nu_\tau$ decays. $\mathcal{B}$ and $d\mathcal{B}/ds$ are in unit of 10^{-4}.

For each RPV coupling product, we can present the correlations of $\mathcal{B}$ and Γ_L^V/Γ_T^V within the constrained parameter space displayed in Fig. 5 by the three-dimensional scatter plots. The differential branching ratio $d\mathcal{B}/ds$ and the normalized FB asymmetry $\bar{\mathcal{A}}_{\rm FB}$ can be shown by the two-dimensional scatter plots. The RPV coupling $\lambda'^{*}_{33i}\lambda'_{31i}$ or $\lambda^{*}_{i33}\lambda'_{i13}$ contributions to $B_u^+ \to \pi^0(\rho^0)\tau^+\nu_\tau$, $B_d^0 \to \pi^-(\rho^-)\tau^+\nu_\tau$, and $B_s^0 \to K^-(K^{*-})\tau^+\nu_\tau$ are also very similar to each other. So we will take an example for $B_d^0 \to \pi^-(\rho^-)\tau^+\nu_\tau$ decay to illustrate the RPV coupling effects. The effects of the RPV couplings $\lambda'^{*}_{33i}\lambda'_{31i}$ and $\lambda^{*}_{i33}\lambda'_{i13}$ on $B_d^0 \to \pi^-(\rho^-)\tau^+\nu_\tau$ decays are shown in Figs. 6 and 7, respectively.

Now we turn to discuss plots of Fig. 6 in detail. The three-dimensional scatter plots Figs. 6(a) and 6(b) show $\mathcal{B}(B_d^0 \to \pi^-(\rho^-)\tau^+\nu_\tau)$ correlated with $|\lambda'^{*}_{33i}\lambda'_{31i}|$ and its phase $\phi_{\not R_p}$. We also give projections to three perpendicular planes, where the $|\lambda'^{*}_{33i}\lambda'_{31i}|$-$\phi_{\not R_p}$ plane displays the constrained regions of $\lambda'^{*}_{33i}\lambda'_{31i}$, as the first plot of Fig. 5. It is shown that $\mathcal{B}(B_d^0 \to \pi^-(\rho^-)\tau^+\nu_\tau)$ has some sensitivity to $|\lambda'^{*}_{33i}\lambda'_{31i}|$ on the $\mathcal{B}(B_d^0 \to \pi^-(\rho^-)\tau^+\nu_\tau)$-$|\lambda'^{*}_{33i}\lambda'_{31i}|$ plane. However, from the $\mathcal{B}(B_d^0 \to \pi^-(\rho^-)\tau^+\nu_\tau)$-$\phi_{\not R_p}$ plane, we see that $\mathcal{B}(B_d^0 \to \pi^-(\rho^-)\tau^+\nu_\tau)$ is very insensitive to $|\phi_{\not R_p}|$. As shown in Fig. 6(e) and 6(f), $\bar{\mathcal{A}}_{\rm FB}(B_d^0 \to \pi^-\tau^+\nu_\tau)$ and $\bar{\mathcal{A}}_{\rm FB}(B_d^0 \to \rho^-\tau^+\nu_\tau)$ are not obviously affected by squark exchange coupling $\lambda'^{*}_{33i}\lambda'_{31i}$, too. In Fig. 6(c), 6(e), and 6(d), the $\lambda'^{*}_{33i}\lambda'_{31i}$ contributions to $d\mathcal{B}(B_d^0 \to \pi^-(\rho^-)\tau^+\nu_\tau)/ds$ are possibly distinguishable from the SM expectations at all s regions.

Figure 7 illustrates the $\lambda^{*}_{i33}\lambda'_{i13}$ contributions to $B_d^0 \to \pi^-(\rho^-)\tau^+\nu_\tau$ decays. $\mathcal{B}(B_d^0 \to \pi^-\tau^+\nu_\tau)$, $\mathcal{B}(B_d^0 \to \rho^-\tau^+\nu_\tau)$, and $\frac{\Gamma_L}{\Gamma_T}(B_d^0 \to \rho^-\tau^+\nu_\tau)$ are all decreasing with $|\lambda^{*}_{i33}\lambda'_{i13}|$, as shown in Fig. 7(a)–7(c). From Fig. 7(f) and 7(g), the effect of $\lambda^{*}_{i33}\lambda'_{i13}$ could allow that $\bar{\mathcal{A}}_{\rm FB}(B_d^0 \to \pi^-\tau^+\nu_\tau)$ and $\bar{\mathcal{A}}_{\rm FB}(B_d^0 \to \rho^-\tau^+\nu_\tau)$ have smaller values and, especially, the sign of $\bar{\mathcal{A}}_{\rm FB}(B_d^0 \to \pi^-\tau^+\nu_\tau)$ could be changed by the effect. There is similar reason for signifi-

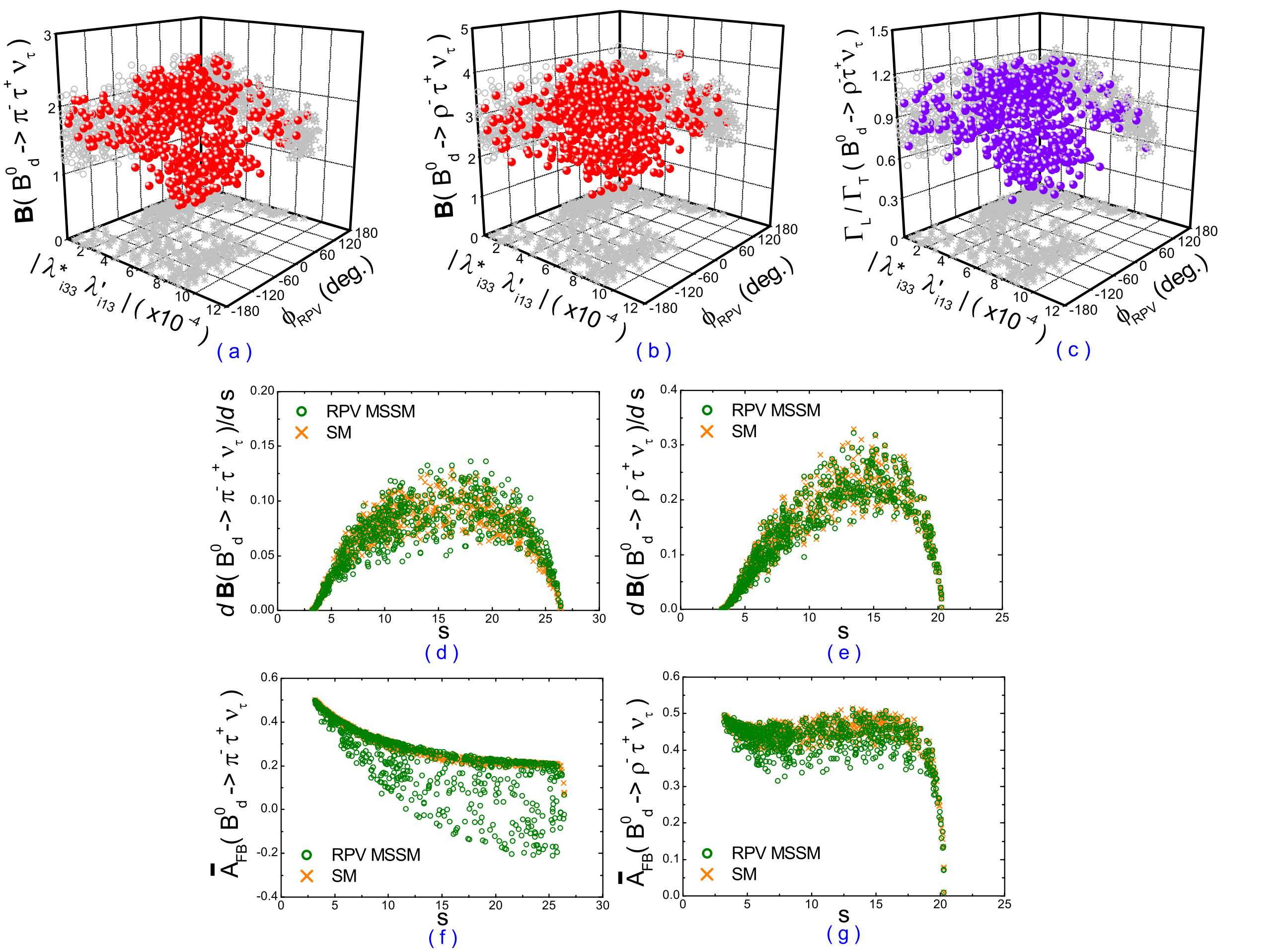

FIG. 7 (color online). The effects of RPV coupling $\lambda^{*}_{i33}\lambda'_{i13}$ on $B_d^0 \to \pi^-(\rho^-)\tau^+\nu_\tau$ decays. $\mathcal{B}$ and $d\mathcal{B}/ds$ are in unit of 10^{-4}.

TABLE VII. The experimental data for the exclusive $\bar{b} \to \bar{u}\ell'^+ \nu_{\ell'}$ decays [24,32–37] and corresponding SM predictions.

	Experimental data	SM value for $\ell' = \mu$	SM value for $\ell' = e$
$\mathcal{B}(B_u^+ \to \mu^+ \nu_\mu)$	$<1.7 \times 10^{-6}$ 90% C.L.	$[2.69, 5.30] \times 10^{-7}$	
$\mathcal{B}(B_u^+ \to e^+ \nu_e)$	$<9.8 \times 10^{-7}$ 90% C.L.		$[6.28, 12.46] \times 10^{-12}$
$\mathcal{B}(B_u^+ \to \pi^0 \ell'^+ \nu_{\ell'})$	$(0.75 \pm 0.09) \times 10^{-4}$	$[0.76, 1.75] \times 10^{-4}$	$[0.75, 1.75] \times 10^{-4}$
$\mathcal{B}(B_d^0 \to \pi^- \ell'^+ \nu_{\ell'})$	$(1.41 \pm 0.08) \times 10^{-4}$	$[1.41, 3.25] \times 10^{-4}$	$[1.40, 3.27] \times 10^{-4}$
$\mathcal{B}(B_u^+ \to \rho^0 \ell'^+ \nu_{\ell'})$	$(1.28 \pm 0.18) \times 10^{-4}$	$[1.49, 4.32] \times 10^{-4}$	$[1.48, 4.45] \times 10^{-4}$
$\mathcal{B}(B_d^0 \to \rho^- \ell'^+ \nu_{\ell'})$	$(2.2 \pm 0.4) \times 10^{-4}$	$[2.78, 8.02] \times 10^{-4}$	$[2.77, 8.32] \times 10^{-4}$

cant effects of slepton exchange on $\bar{\mathcal{A}}_{\rm FB}(B \to P\tau^+\nu_\tau)$ as Fig. 4(f), *i.e.* the normalized FB asymmetry is not suppressed by m_ℓ^2 and s. The different effects between the charged Higgs and slepton exchange on $\bar{\mathcal{A}}_{\rm FB}(B \to P\tau^+\nu_\tau)$, shown in Fig. 4(f) and 7(f), come from the RPV weak phase $\phi_{\not R_p}$ and the CKM weak phase γ. The weak phases contribute only to the RPV MSSM predictions of $\bar{\mathcal{A}}_{\rm FB}(B \to P\tau^+\nu_\tau)$.

B. The exclusive $b \to u\ell'\nu_{\ell'}(\ell' = \mu$ or $e)$ decays

For the exclusive $b \to u\ell'\nu_{\ell'}$ decays, several branching ratios have been accurately measured by *BABAR*, Belle, and CLEO [32–37]. Their averaged values from the particle data group [24] and corresponding SM prediction values are given in Table VII. The experimental results are roughly consistent with the SM predictions; nevertheless there are still windows for NP in these processes. Because many branching ratios have been accurately measured, in order to easily obtain the solution of the RPV coupling products, we will use the experimental data given in Table VII, which are varied randomly within 2σ range to constrain the RPV coupling products.

Four RPV coupling products $\lambda'^*_{23i}\lambda'_{21i}$, $\lambda^*_{i22}\lambda'_{i13}$ for $\ell' = \mu$ and $\lambda'^*_{13i}\lambda'_{11i}$, $\lambda^*_{i11}\lambda'_{i13}$ for $\ell' = e$ are related to 14 exclusive $b \to u\ell'^+\nu_{\ell'}$ decay modes. We use $\mathcal{B}(B_u^+ \to \ell'^+\nu_{\ell'})$, $\mathcal{B}(B_d^0 \to \pi^-(\rho^-)\ell'^+\nu_{\ell'})$, $\mathcal{B}(B_u^+ \to \pi^+(\rho^+)\ell'^+\nu_{\ell'})$, and their experimental data listed in Table VII to restrict the relevant RPV parameter spaces. The random variation of the parameters subjected to the constraints as discussed above leads to the scatter plots displayed in Fig. 8. In Fig. 8, the RPV weak phases of the slepton exchange couplings $\lambda^*_{i22}\lambda'_{i13}$ and $\lambda^*_{i11}\lambda'_{i13}$ have the entirely allowed ranges $[-180°, 180°]$, but for every RPV weak phase of the squark exchange couplings $\lambda'^*_{23i}\lambda'_{21i}$ and $\lambda'^*_{13i}\lambda'_{11i}$, there are two possible bands. For $\lambda'^*_{23i}\lambda'_{21i}$, one band of its phase is $\phi_{\not R_p} \in [-180°, -129°]$; another is $\phi_{\not R_p} \in [-61°, 180°]$. And for

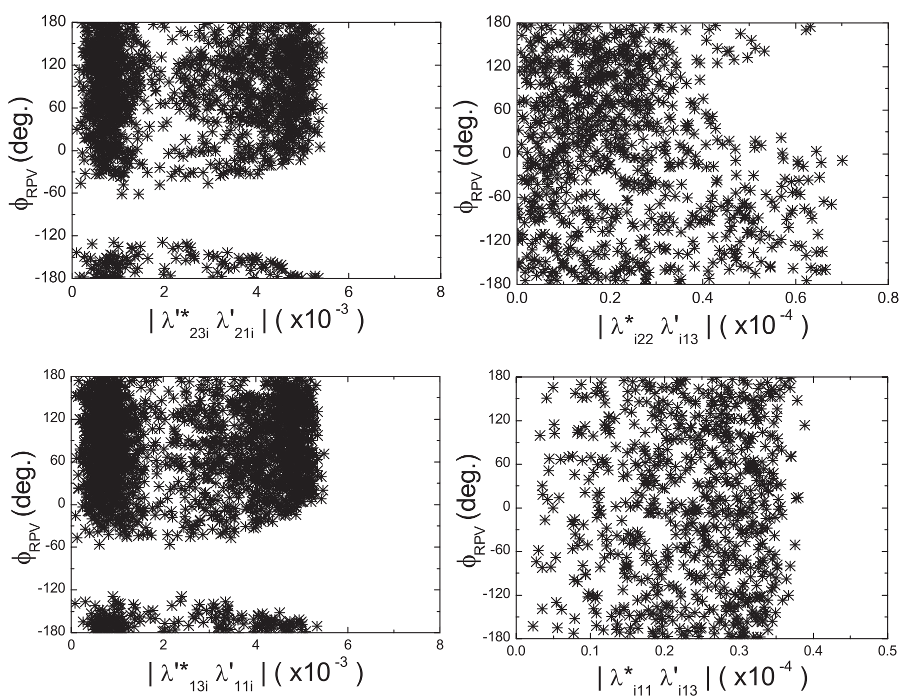

FIG. 8. The allowed parameter spaces for the relevant RPV coupling products constrained by the measurements of the exclusive $\bar{b} \to \bar{u}\ell'^+\nu_{\ell'}$ decays listed in Table VII.

TABLE VIII. Bounds for the relevant RPV coupling products by the exclusive $\bar{b} \to \bar{u}\ell'^+\nu_{\ell'}$ decays for 100 GeV sfermions, and previous bounds are listed for comparison [30,31,38].

Couplings	Bounds [Processes]	Previous bounds
$\lvert\lambda'^*_{23i}\lambda'_{21i}\rvert$	$\leq 5.44\times10^{-3}[^{B_u^+\to\mu^+\nu_\mu}_{B\to M'\mu^+\nu_\mu}]$	$\leq 2.64\times10^{-3}$
$\lvert\lambda^*_{i22}\lambda'_{i13}\rvert$	$\leq 7.00\times10^{-5}[^{B_u^+\to\mu^+\nu_\mu}_{B\to M'\mu^+\nu_\mu}]$	$\leq 3.24\times10^{-3}$
$\lvert\lambda'^*_{13i}\lambda'_{11i}\rvert$	$\leq 5.49\times10^{-3}[^{B_u^+\to e^+\nu_e}_{B\to M'e^+\nu_e}]$	$\leq 5.4\times10^{-3}$
$\lvert\lambda^*_{i11}\lambda'_{i13}\rvert$	$\leq 3.88\times10^{-5}[^{B_u^+\to e^+\nu_e}_{B\to M'e^+\nu_e}]$	$\leq 2.89\times10^{-3}(i=2)$ $\leq 6.82\times10^{-3}(i=3)$

$\lambda'^*_{13i}\lambda'_{11i}$, one band is $\phi_{\not{R}_p} \in [-180°, -129°]$; another is $\phi_{\not{R}_p} \in [-56°, 180°]$. The magnitudes of the squark and slepton exchange couplings have been upper limited. The upper limits are summarized in Table VIII. Compared with the existing bounds [30,31,38], which are estimated from the products of the smallest values of two single couplings, we get quite strong quadric bounds on $|\lambda^*_{i22}\lambda'_{i13}|$ and $|\lambda^*_{i11}\lambda'_{i13}|$, due to the slepton exchange couplings.

Using the constrained parameter spaces shown in Fig. 8, we predict the RPV effects on other quantities which have not been measured yet in the exclusive $\bar{b} \to \bar{u}\ell'^+\nu_{\ell'}$ decays. Our predictively numerical results are summarized in Table IX. Because the RPV effects on the exclusive $\bar{b} \to \bar{u}\mu^+\nu_\mu$ and $\bar{b} \to \bar{u}e^+\nu_e$ are quite similar, as shown in Table IX, here we give their remarks altogether:

(1) For the squark exchange couplings $\lambda'^*_{g3i}\lambda'_{g1i}$, their effects can decrease the upper limits and lower limits of $\mathcal{B}(B_u^+ \to \ell'^+\nu_{\ell'})$, $\mathcal{B}(B_s^0 \to K^-\ell'^+\nu_{\ell'})$, and $\mathcal{B}(B_s^0 \to K^{*-}\ell'^+\nu_{\ell'})$, as well as shrink the allowed ranges of these branching ratios. The squark exchange effects are completely canceled in $\frac{\Gamma_L}{\Gamma_T}(B \to V\ell'^+\nu_{\ell'})$.

(2) The slepton exchange couplings $\lambda^*_{igg}\lambda'_{i13}$, which satisfy all present experimental constraints, could significantly change the purely leptonic decay branching ratios $\mathcal{B}(B_u^+ \to \ell'^+\nu_{\ell'})$: They could enhance the ratios to their experimental upper limits. $\mathcal{B}(B_u^+ \to \mu^+\nu_\mu)$ could be suppressed to 10^{-9} or enhanced to order of 10^{-6}, and $\mathcal{B}(B_u^+ \to e^+\nu_e)$ could be enhanced 5 orders from order of 10^{-12} to order of 10^{-7}. The reason for these significant effects on $\mathcal{B}(B_u^+ \to \ell'^+\nu_{\ell'})$ is that the SM effective Hamiltonian is proportional to $(\bar{b}\gamma_\mu(1-\gamma_5)u) \times (\bar{\nu}_{\ell'}\gamma^\mu(1-\gamma_5)\ell')$, whose contribution to $\mathcal{B}(B_u^+ \to \ell'^+\nu_{\ell'})$ is suppressed by $m^2_{\ell'}$ due to helicity suppression, while the effective Hamiltonian of slepton exchange is proportional to $(\bar{b}(1-\gamma_5)u)(\bar{\nu}_{\ell'}(1+\gamma_5)\ell')$, whose contribution is not suppressed by $m^2_{\ell'}$. Therefore, compared with the SM contribution, the slepton exchange couplings have great effects on $\mathcal{B}(B_u^+ \to \ell'^+\nu_{\ell'})$. The allowed ranges of $\mathcal{B}(B_s^0 \to K^-(K^{*-})\ell'^+\nu_{\ell'})$ and $\frac{\Gamma_L}{\Gamma_T}(B \to V\ell'^+\nu_{\ell'})$ are shrunken by $\lambda^*_{igg}\lambda'_{i13}$ couplings.

Figures 9 and 10 show the RPV contributions in the $\bar{b} \to \bar{u}\mu^+\nu_\mu$ decays. We view that the trends in the changes of the physical observables with the modulus and weak phase $\phi_{\not{R}_p}$ of the RPV couplings by the three-dimensional scatter plots, and we also compare the SM predictions with the RPV MSSM predictions in $d\mathcal{B}/ds$ and $\bar{\mathcal{A}}_{\rm FB}$ by the two-dimensional scatter plots. Figure 9 displays the $\lambda'^*_{23i}\lambda'_{21i}$ effects due to the squark exchange couplings on the exclusive $\bar{b} \to \bar{u}\mu^+\nu_\mu$ decays. From Fig. 9(d) and 9(e), we find the contributions of $\lambda'^*_{23i}\lambda'_{21i}$ can suppress $d\mathcal{B}(B_s^0 \to K^-\mu^+\nu_\mu)/ds$ and $d\mathcal{B}(B_s^0 \to K^{*-}\mu^+\nu_\mu)/ds$, so their contributions are easily distinguishable from the SM predictions with theoretical uncertainties included. However, these contributions to other observables are small, and

TABLE IX. The theoretical predictions for CP averaged $\mathcal{B}$ and Γ^V_L/Γ^V_T of the exclusive $\bar{b} \to \bar{u}\ell'^+\nu_{\ell'}$ decays in the SM and the RPV MSSM. The RPV MSSM predictions are obtained by the constrained regions of the different RPV coupling products. The index $g=1$ and 2 for $\ell' = e$ and μ, respectively.

	SM value	MSSM value w/$\lambda'^*_{g3i}\lambda'_{g1i}$	MSSM value w/$\lambda^*_{igg}\lambda'_{i13}$
$\mathcal{B}(B_u^+ \to \mu^+\nu_\mu)$	$[2.69, 5.30]\times10^{-7}$	$[1.55, 3.64]\times10^{-7}$	$[0.03, 16.98]\times10^{-7}$
$\mathcal{B}(B_s^0 \to K^-\mu^+\nu_\mu)$	$[1.98, 4.81]\times10^{-4}$	$[1.14, 3.07]\times10^{-4}$	$[2.00, 3.45]\times10^{-4}$
$\mathcal{B}(B_s^0 \to K^{*-}\mu^+\nu_\mu)$	$[3.17, 8.99]\times10^{-4}$	$[1.99, 5.14]\times10^{-4}$	$[3.17, 6.43]\times10^{-4}$
$\frac{\Gamma_L}{\Gamma_T}(B_u^+ \to \rho^0\mu^+\nu_\mu)$	[0.49, 1.52]	$\cdots$	[0.54, 0.66]
$\frac{\Gamma_L}{\Gamma_T}(B_d^0 \to \rho^+\mu^+\nu_\mu)$	[0.49, 1.52]	$\cdots$	[0.54, 0.66]
$\frac{\Gamma_L}{\Gamma_T}(B_s^0 \to K^{*-}\mu^+\nu_\mu)$	[0.68, 1.70]	$\cdots$	[0.71, 1.63]
$\mathcal{B}(B_u^+ \to e^+\nu_e)$	$[6.26, 12.37]\times10^{-12}$	$[3.49, 8.60]\times10^{-12}$	$[6.26\times10^{-12}, 9.8\times10^{-7}]$
$\mathcal{B}(B_s^0 \to K^-e^+\nu_e)$	$[1.99, 4.78]\times10^{-4}$	$[1.15, 3.07]\times10^{-4}$	$[2.01, 3.43]\times10^{-4}$
$\mathcal{B}(B_s^0 \to K^{*-}e^+\nu_e)$	$[3.19, 8.96]\times10^{-4}$	$[1.89, 5.22]\times10^{-4}$	$[3.29, 6.41]\times10^{-4}$
$\frac{\Gamma_L}{\Gamma_T}(B_u^+ \to \rho^0e^+\nu_e)$	[0.48, 1.53]	$\cdots$	[0.53, 0.66]
$\frac{\Gamma_L}{\Gamma_T}(B_d^0 \to \rho^+e^+\nu_e)$	[0.48, 1.53]	$\cdots$	[0.53, 0.66]
$\frac{\Gamma_L}{\Gamma_T}(B_s^0 \to K^{*-}e^+\nu_e)$	[0.69, 1.68]	$\cdots$	[0.73, 1.67]

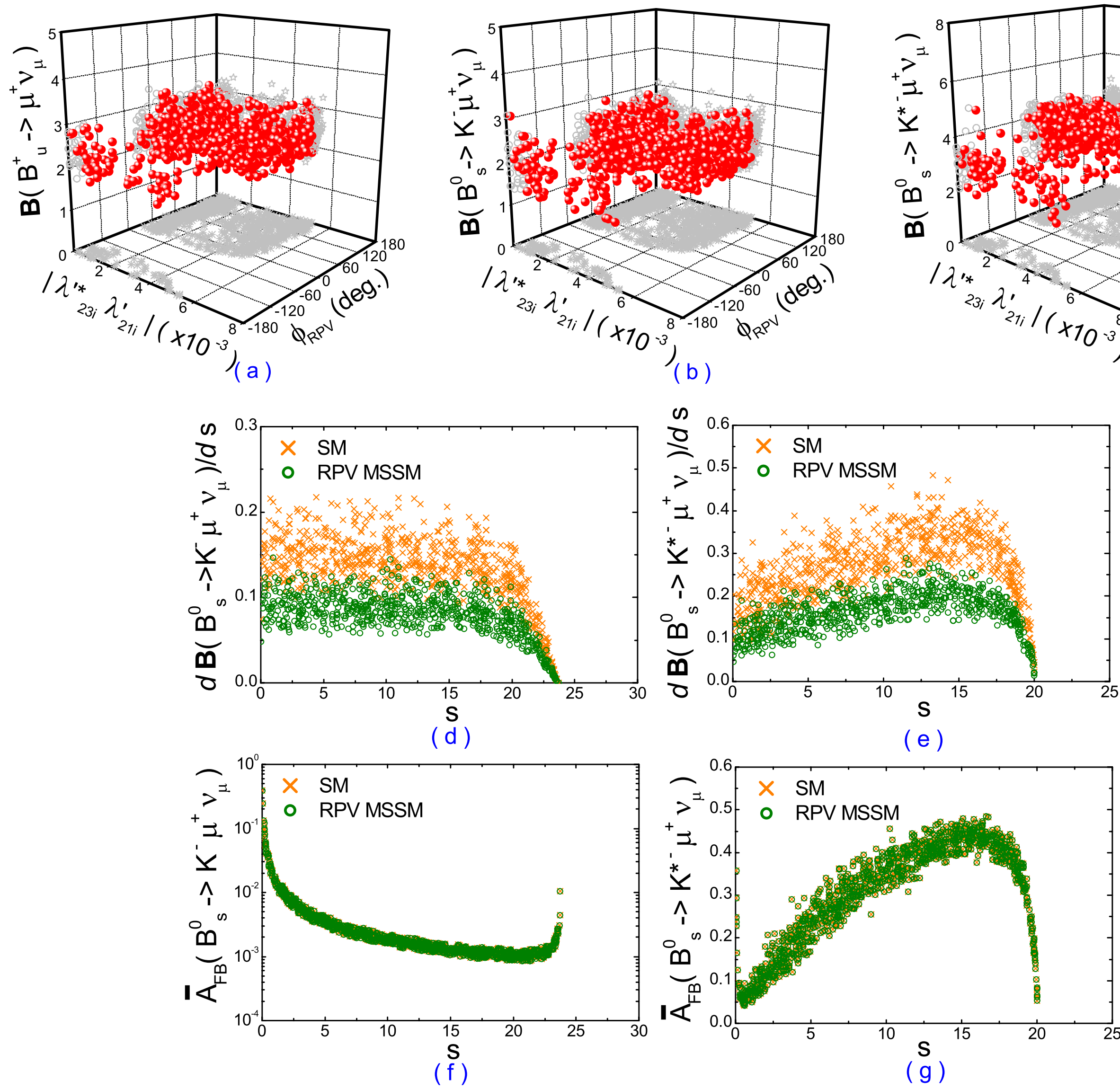

FIG. 9 (color online). The effects of RPV coupling $\lambda'^*_{23i}\lambda'_{21i}$ on the exclusive $\bar{b} \to \bar{u}\mu^+\nu_\mu$ decays. $\mathcal{B}$ and $d\mathcal{B}/ds$ of the semileptonic decays are in unit of 10^{-4}, and $\mathcal{B}(B_u^+ \to \mu^+\nu_\mu)$ is in unit of 10^{-7}.

we cannot find visible effects on $\mathcal{B}(B_u^+ \to \mu^+\nu_\mu)$, $\mathcal{B}(B_s^0 \to K^-\mu^+\nu_\mu)$, $\mathcal{B}(B_s^0 \to K^{*-}\mu^+\nu_\mu)$, $\bar{\mathcal{A}}_{\rm FB}(B_s^0 \to K^-\mu^+\nu_\mu)$, and $\bar{\mathcal{A}}_{\rm FB}(B_s^0 \to K^{*-}\mu^+\nu_\mu)$. Figure 10 presents the $\lambda^*_{i22}\lambda'_{i13}$ effects due to the slepton exchange couplings on the exclusive $\bar{b} \to \bar{u}\mu^+\nu_\mu$ decays. The three-dimensional scatter plot Fig. 10(a) shows $\mathcal{B}(B_u^+ \to \mu^+\nu_\mu)$ correlated with $|\lambda^*_{i22}\lambda'_{i13}|$ and its phase $\phi_{\not R_p}$, so we can see that $\mathcal{B}(B_u^+ \to \mu^+\nu_\mu)$ is greatly increased with $|\lambda^*_{i22}\lambda'_{i13}|$, but is insensitive to ϕ_{R_p}. From Fig. 10(i), we find $\lambda^*_{i22}\lambda'_{i13}$ coupling contributions to $\bar{\mathcal{A}}_{\rm FB}(B_s^0 \to K^-\mu^+\nu_\mu)$ are possibly large. There are not obvious $\lambda^*_{i22}\lambda'_{i13}$ coupling effects, overlapping with the SM results in $\mathcal{B}(B_s^0 \to K^-\mu^+\nu_\mu)$, $\mathcal{B}(B_s^0 \to K^{*-}\mu^+\nu_\mu)$, $\frac{\Gamma_L}{\Gamma_T}(B \to V\mu^+\nu_\mu)$, $d\mathcal{B}(B_s^0 \to K^-\mu^+\nu_\mu)/ds$, $d\mathcal{B}(B_s^0 \to K^{*-}\mu^+\nu_\mu)/ds$, and $\bar{\mathcal{A}}_{\rm FB}(B_s^0 \to K^{*-}\mu^+\nu_\mu)$.

For the exclusive $\bar{b} \to \bar{u}e^+\nu_e$ decays, the effects of $\lambda^*_{i11}\lambda'_{i13}$ on $\bar{\mathcal{A}}_{\rm FB}(B_s^0 \to K^-e^+\nu_e)$ can be distinguishible from the SM prediction, but both the SM prediction and the RPV MSSM prediction are too small to be accessible at LHC.

VI. SUMMARY

In this paper, we have studied the 21 decay channels $B_u^+ \to \ell^+\nu_\ell$, $B_u^+ \to \pi^0\ell^+\nu_\ell$, $B_d^0 \to \pi^-\ell^+\nu_\ell$, $B_s^0 \to K^-\ell^+\nu_\ell$, $B_u^+ \to \rho^0\ell^+\nu_\ell$, $B_d^0 \to \rho^-\ell^+\nu_\ell$, and $B_s^0 \to K^{*-}\ell^+\nu_\ell$ $(\ell = \tau, \mu, e)$ in the MSSM with and without R_p violation. Considering the theoretical uncertainties and the experimental errors, we have obtained fairly constrained parameter spaces of new physics coupling constants from the present experimental data. Furthermore, we have predicted the charged Higgs effects and the RPV

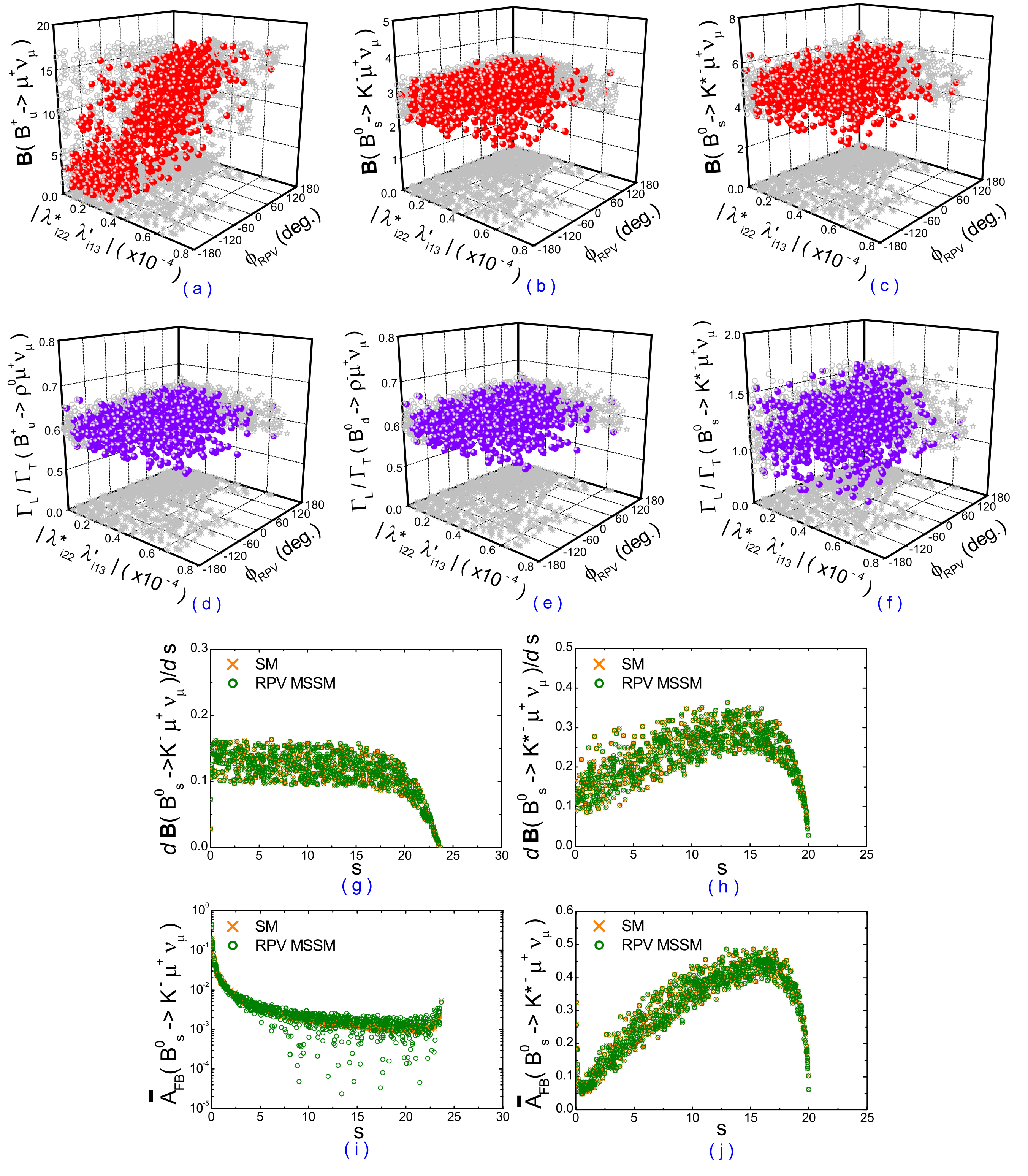

FIG. 10 (color online). The effects of RPV coupling $\lambda^*_{i22}\lambda'_{i13}$ on the exclusive $\bar{b} \to \bar{u}\mu^+\nu_\mu$ decays. $\mathcal{B}$ and $d\mathcal{B}/ds$ of the semileptonic decays are in unit of 10^{-4}, and $\mathcal{B}(B_u^+ \to \mu^+\nu_\mu)$ is in unit of 10^{-7}.

effects on the branching ratios, the normalized FB asymmetries of charged leptons and the ratios of longitudinal to transverse polarization of the vector mesons, which have not been measured or have not been well measured yet.

We have found that both the charged Higgs coupling and the slepton exchange coupling $\lambda^*_{i33}\lambda'_{i13}$ have significant effects on $\bar{\mathcal{A}}_{\rm FB}(B \to P\tau^+\nu_\tau)$, and the sign of $\bar{\mathcal{A}}_{\rm FB}(B \to P\tau^+\nu_\tau)$ could be changed by these effects. The charged Higgs effects and the slepton exchange coupling effects are distinguishable in the purely leptonic $B^+_u \to \mu^+\nu_\mu, e^+\nu_e$ decays. The charged Higgs coupling has negligible effects on $\mathcal{B}(B^+_u \to \mu^+\nu_\mu)$ and $\mathcal{B}(B^+_u \to e^+\nu_e)$, but the slepton exchange contributions of the RPV MSSM are very sensitive to $\mathcal{B}(B^+_u \to \mu^+\nu_\mu)$ and $\mathcal{B}(B^+_u \to e^+\nu_e)$. If the enhancement of branching ratios is not discovered in $B^+ \to \mu^+\nu_\mu$, $e^+\nu_e$ decays, the new limits from future experiments would constrain the slepton exchange couplings. Otherwise, it would imply that RPV effects are likely to be seen. We have also compared the SM predictions with the RPV predictions of $d\mathcal{B}/ds$ and $\bar{\mathcal{A}}_{\rm FB}$ in $B \to P(V)\ell^+\nu_\ell$ decays. We have found that the RPV couplings due to squark exchange are in principle distinguishable from the SM contributions at all kinematic regions in all 18 semileptonic $d\mathcal{B}/ds$. The results in this paper could be useful for probing the charged Higgs effects and the RPV MSSM effects, and will correlate strongly with searches for the direct supersymmetric signals at future experiments, for example, LHC and super-B factories.

[1] J. F. Gunion, H. E. Haber, G. L. Kane, and S. Dawson, *The Higgs Hunters Guide* (Addison-Wesley, Menlo-Park, 1990); see also: (E) SCIPP-92-58, arXiv:hep-ph/9302272.

[2] P. Fayet, Nucl. Phys. **B90**, 104 (1975); Phys. Lett. **64B**, 159 (1976); **69B**, 489 (1977); **84B**, 416 (1979).

[3] K. Inoue, A. Komatsu, and S. Takeshita, Prog. Theor. Phys. **68**, 927 (1982); **70**, 330(E) (1983); H. Nilles, Phys. Rep. **110**, 1 (1984); H. Haber and G. Kane, Phys. Rep. **117**, 75 (1985).

[4] Y. Grossman and Z. Ligeti, Phys. Lett. B **332**, 373 (1994); K. S. Babu and C. Kolda, Phys. Rev. Lett. **84**, 228 (2000).

[5] C. S. Huang, W. Liao, and Q. S. Yan, Phys. Rev. D **59**, 011701 (1998); C. S. Huang, L. Wei, Q. S. Yan, and S. H. Zhu, Phys. Rev. D **63**, 114021 (2001); **64**, 059902 (2001).

[6] P. H. Chankowski and Ł. Sławianowska, Phys. Rev. D **63**, 054012 (2001); C. Bobeth, T. Ewerth, F. Krüger, and J. Urban, Phys. Rev. D **64**, 074014 (2001).

[7] G. D'Ambrosio, G. F. Giudice, G. Isidori, and A. Strumia, Nucl. Phys. **B645**, 155 (2002); A. J. Buras, P. H. Chankowski, J. Rosiek, and Ł. Sławianowska, Phys. Lett. B **546**, 96 (2002); G. Isidori and A. Retico, J. High Energy Phys. 09 (2002) 063.

[8] C. Bobeth, T. Ewerth, F. Krüger, and J. Urban, Phys. Rev. D **66**, 074021 (2002); T. Ibrahim and P. Nath, Phys. Rev. D **67**, 016005 (2003).

[9] F. Borzumati, C. Greub, and Y. Yamada, Phys. Rev. D **69**, 055005 (2004); S. Baek, Phys. Lett. B **595**, 461 (2004).

[10] M. S. Carena, A. Menon, R. Noriega-Papaqui, A. Szynkman, and C. E. M. Wagner, Phys. Rev. D **74**, 015009 (2006); E. Lunghi, W. Porod, and O. Vives, Phys. Rev. D **74**, 075003 (2006); J. Ellis, S. Heinemeyer, K. A. Olive, A. M. Weber, and G. Weiglein, J. High Energy Phys. 08 (2007) 083.

[11] A. J. Buras, P. H. Chankowski, J. Rosiek, and Ł. Sławianowska, Nucl. Phys. **B659**, 3 (2003).

[12] W. S. Hou, Phys. Rev. D **48**, 2342 (1993); G. Isidori and P. Paradisi, Phys. Lett. B **639**, 499 (2006).

[13] G. R. Farrar and P. Fayet, Phys. Lett. **76B**, 575 (1978).

[14] J. H. Jang, Y. G. Kim, and J. S. Lee, Phys. Lett. B **408**, 367 (1997); J. H. Jang, Y. G. Kim, and J. S. Lee, Phys. Rev. D **58**, 035006 (1998); G. Bhattacharyya and A. Raychaudhuri, Phys. Rev. D **57**, R3837 (1998).

[15] G. Bhattacharyya and A. Datta, Phys. Rev. Lett. **83**, 2300 (1999); D. Chakraverty and D. Choudhury, Phys. Rev. D **63**, 075009 (2001); B. Dutta, C. S. Kim, and S. Oh, Phys. Lett. B **535**, 249 (2002).

[16] A. Datta, Phys. Rev. D **66**, 071702 (2002); B. Dutta, C. S. Kim, and S. Oh, Phys. Rev. Lett. **90**, 011801 (2003); J. P. Saha and A. Kundu, Phys. Rev. D **66**, 054021 (2002).

[17] B. Dutta, C. S. Kim, S. Oh, and G. H. Zhu, Eur. Phys. J. C **37**, 273 (2004); B. Dutta, C. S. Kim, S. Oh, and G. H. Zhu, Phys. Lett. B **601**, 144 (2004); Y. D. Yang, R. M. Wang, and G. R. Lu, Phys. Rev. D **72**, 015009 (2005).

[18] R. Wang, G. R. Lu, E. K. Wang, and Y. D. Yang, Eur. Phys. J. C **47**, 815 (2006); S. Nandi and J. P. Saha, Phys. Rev. D **74**, 095007 (2006); Y. G. Xu, R. M. Wang, and Y. D. Yang, Phys. Rev. D **74**, 114019 (2006).

[19] H. K. Dreiner, M. Krämer, and B. O'leary, Phys. Rev. D **75**, 114016 (2007); A. Mir and F. Tahir, arXiv:0707.2268; J. J. Wang, R. M. Wang, Y. G. Xu, and Y. D. Yang, Phys. Rev. D **77**, 014017 (2008).

[20] S. Baek and Y. G. Kim, Phys. Rev. D **60**, 077701 (1999); H. Dreiner, G. Polesello, and M. Thormeier, Phys. Rev. D **65**, 115006 (2002).

[21] S. Weinberg, Phys. Rev. D **26**, 287 (1982).

[22] P. Ball and R. Zwicky, Phys. Rev. D **71**, 014015 (2005); Phys. Rev. D **71**, 014029 (2005).

[23] J. G. Körner and G. A. Schuler, Phys. Lett. B **226**, 185 (1989).

[24] W. M. Yao *et al.*, J. Phys. G **33**, 1 (2006) and 2007 partial update for edition 2008.

[25] Heavy Flavor Averaging Group, http://www.slac.stanford.edu/xorg/hfag.

[26] C. H. Chen and C. Q. Geng, J. High Energy Phys. 10 (2006) 053.

[27] B. Aubert *et al.* (*BABAR* Collaboration), Phys. Rev. D **76**, 052002 (2007).

[28] K. Ikado *et al.* (Belle Collaboration), Phys. Rev. Lett. **97**,

251802 (2006).
[29] A. G. Akeroyd and S. Recksiegel, J. Phys. G **29**, 2311 (2003).
[30] M. Chemtob, Prog. Part. Nucl. Phys. **54**, 71 (2005).
[31] R. Barbier *et al.*, Phys. Rep. **420**, 1 (2005).
[32] T. Hokuue *et al.* (Belle Collaboration), Phys. Lett. B **648**, 139 (2007).
[33] B. Aubert *et al.* (*BABAR* Collaboration), Phys. Rev. Lett. **98**, 091801 (2007).
[34] B. Aubert *et al.* (*BABAR* Collaboration), Phys. Rev. Lett. **97**, 211801 (2006).
[35] B. Aubert *et al.* (*BABAR* Collaboration), Phys. Rev. D **72**, 051102(R) (2005).
[36] B. H. Behrens *et al.* (CLEO Collaboration), Phys. Rev. D **61**, 052001 (2000).
[37] S. B. Athar *et al.* (CLEO Collaboration), Phys. Rev. D **68**, 072003 (2003).
[38] B. C. Allanach, A. Dedes, and H. K. Dreiner, Phys. Rev. D **60**, 075014 (1999).